Full 3D homogenization approach to investigate the behavior of masonry arch bridges: The Venice trans-lagoon railway bridge

E. Reccia [a], G. Milani [b,*], A. Cecchi [a], A. Tralli [c]

[a] *IUAV University of Venice, Italy*
[b] *Technical University in Milan, Italy*
[c] *University of Ferrara, Italy*

Received 24 January 2014
Received in revised form 29 April 2014
Accepted 31 May 2014

1. Introduction

The Italian railroad network includes thousands of masonry arch bridges, mainly built during the XIX century, that are still in exercise. This is also common in other European countries, such as UK, France, Spain and Germany [1]. The European railway network has been almost completely built in one century, from the 1825, year of the first railway, to the 30's of the twentieth century. The first Italian railway has been realized in 1839 and the great part of bridges have been built in the fifty years from 1860 to 1910, subsequently to the unification of Italy. Thanks to their mechanical properties, thousands of masonry arch railway bridges

* Corresponding author.
E-mail addresses: gabriele.milani@polimi.it, gabriele.milani77@gmail.com (G. Milani).

have been built and, thanks to the durability of their materials, a high percentage of them are still in service, Fig. 1.

Increase in transport capacity demand, deterioration of materials and identification of a variety of defects have resulted in the recent past in the need for assessment and maintenance procedures for existing masonry bridges. As a consequence, considerable effort to develop reliable structural models based on a limited number of constitutive parameters has been made.

At present, a large amount of literature regarding the analysis up to collapse of masonry arch bridges and masonry arches in general is present [2–15]. However, such literature focuses almost exclusively on 1D/2D problems. Obviously, such structural models involve varying levels of accuracy and simplifications, which limit their range of applicability to specific cases. The most common idealizations of masonry material behavior are elastic, non-linear elastic and elastic plastic (for a detailed discussion the reader is referred to e.g. [9]), but the most diffused approach, particularly in the case of masonry arch bridges and curved structures in general, still remains limit analysis [5,10–17]. Limit analysis provides very quickly failure mechanisms and an estimation of the load carrying capacity of the structure but for serviceability purposes, as the case here treated is incapable of providing suitable information, as for instance the deflection profile under the design rail/traffic load and the crack maps, i.e. the zones undergoing inelastic deformation.

Besides the historic rules [18], the classic approach to determine the stability of arch bridges is probably due to Pippard and Ashby [19], Pippard [2] and Heyman [20]. Finally, Heyman [20] was the first to extend in a clear and explicit way to masonry arches both the kinematic and static theorems of limit analysis, according to which the structure is safe if a thrust line inner to the arch depth can be determined in equilibrium with the external loads.

The procedure may be handled without computational assistance, and fits well with experimental data for very simple arches without backfill and under specific load conditions. More recent works (e.g. Gilbert and Melbourn [3], Hughes and Blackler [21] and Boothby [4]) are based on a rigid block discretization of the arches within limit analysis concepts coupled with FEs. While such an approach is very appealing because it provides failure mechanisms and load multipliers for a variety of different 2D geometries and loading conditions, still it is based on strong simplifications, which disregard 3D effects and consider the role played by the backfill only in an approximate way.

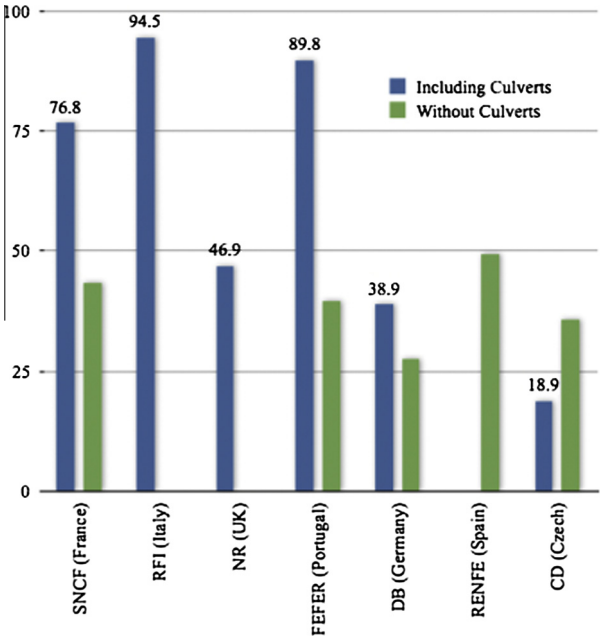

Fig. 1. Proportion in percentage of masonry arch railway bridges on the overall bridge stock of some of the main European railroad network, adapted from [1].

To rigorously investigate the role played by the backfill in the determination of the actual load carrying capacity of 2D bridges, a discretization with plane strain rigid-plastic elements and interfaces is needed, as recently proposed by Cavicchi and Gambarotta [11,12]. While this latter approach is very powerful, giving good predictions of the actual behavior of real bridges, it still has the disadvantage that it cannot be used for the analysis of skewed or straight arches in presence of eccentric loads. Transversal effects may be very important from a practical point of view, playing a crucial role in the decrease of the load bearing capacity and 3D limit analyses models seem still missing in the technical literature, essentially because of the lack of commercial programs and of the prohibitive computational cost required by refined discretizations within standard linear programming algorithms. While limit analysis is a very appealing alternative to common non-linear simulations, it is unable to give any prediction of the pseudo-ductility of the structure, because of the material hypotheses at the base of such formulation (infinite ductility of the constituent materials). To have a prediction on displacements in the non-linear range, non-linear FE approaches (ranging from 1D up to full 3D) have thus been used in the recent past [8,22–24]. For complex geometries, FEs models generally require many elements and variables, making the solution of the incremental problem difficult even for small bridges. In addition, since commercial codes are normally used, it is also difficult to adapt material models available to the actual masonry behavior, to properly take into account the orthotropy along material axes [25,26], softening behavior and separate failure surfaces for tension and compression [27–33].

Two distinct FE software are utilized in the paper to perform several numerical simulations on the Venice trans-lagoon bridge (Fig. 2), namely a macroscopic FE procedure dealing with isotropic elastic–plastic materials within the commercial code Strand7 [34], and a homogenization non-linear FE procedure recently presented in [15,16], which relies into a discretization of the structure with rigid parallelepiped elements and non-linear quadrilateral interfaces. The latter approach allows performing non-linear static simulations taking into account the orthotropic behavior and the softening of actual masonry materials by means of a Sequential Quadratic Programming (SQP) strategy recently presented in detail in [16], where the reader is referred to. When for the interfaces a rigid plastic behavior with infinite ductility is assumed, an upper bound limit analysis can be performed, which allows the estimation of collapse loads and failure mechanisms, by means of the solution of a large scale linear programming problem (LP).

For all models, a full 3D discretization is adopted in order to suitably consider the unsymmetrical response of the structure induced by live loads eccentrically applied and the always present transversal effect due to the three-dimensional geometry, even in presence of loads symmetrically disposed on the width. Furthermore, it is worth noting that the role played by the presence of lateral stone arches on the barrel vault may be estimated only using a full 3D model.

Finally, the stabilizing role of the backfill up the collapse is evaluated together with the effects induced by a foundation vertical settlement of a pile.

In Section 2, the salient features of the different codes used are summarized. In Section 3, the case study examined, namely the trans-lagoon Venice railway bridge, Fig. 2, is presented in detail and the homogenization procedures employed for the barrel vault and the stone arches are also reported. In Section 4 the results of the structural analyses performed both on service loads and at collapse are critically discussed and the effect of backfill and spandrels is highlighted. Finally the effect of the foundation settlement of a pile is presented in Section 5.

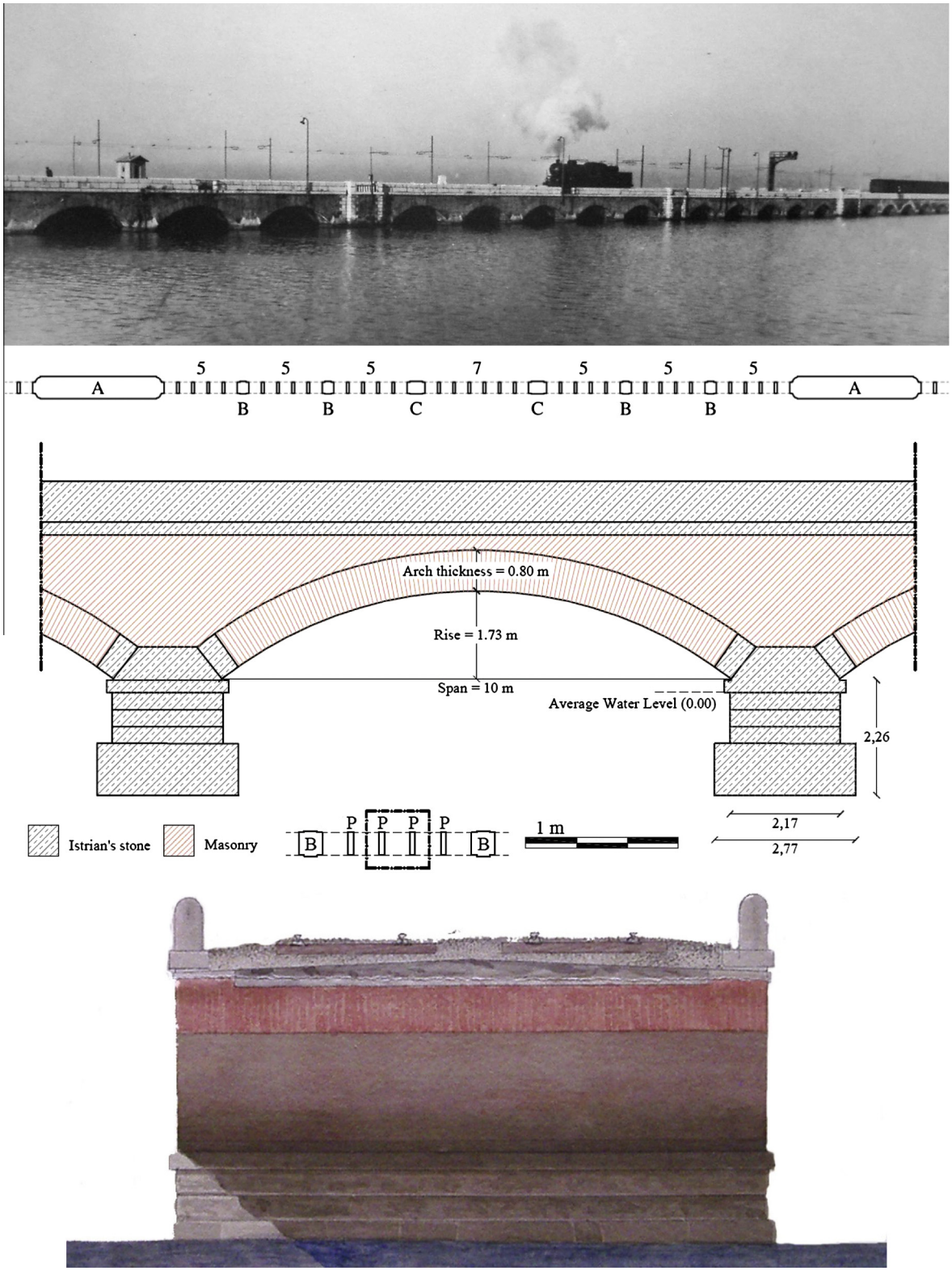

Fig. 2. Historical photograph of the Venetian trans-lagoon bridge. One "stadio" of the bridge with artificial islands on the left and right (A). Dimension of a single arch and transversal section at crown.

2. Modeling strategies

In order to obtain a comprehensive insight into the structural behavior of the bridge, two different FE codes are utilized in the paper to perform the analyses. The first software is a FE commercial code, namely Strand7 [34], whereas the second is a non-commercial software [15,16] specifically conceived for structural analyses in the non-linear range of complex masonry structures. In the following sub-sections, a brief overview of the aforementioned code features are reported.

2.1. Commercial code

Preliminarily, a general purpose commercial FE software is utilized, namely Strand7 [34]. In order to analyze the structure taking into account transversal effects, a discretization with eight-noded parallelepiped elements is arranged. The global behavior of the bridge is investigated in both the linear elastic and non-linear elasto-plastic field. In this framework, two hypotheses of increasing complexity are done on the material behavior. When dealing with linear elastic analyses, utilized to investigate the behavior of the bridge under service loads, either isotropic or orthotropic constitutive relationships are assumed for the different geometric elements of the structure. In particular, when dealing with the barrel vault, spandrels and external arch rings, orthotropic properties derived from rigorous FE homogenization in the elastic range are adopted. For backfill and piers, isotropic properties are assumed.

When dealing with the non-linear simulations, elastic perfectly-plastic materials are assumed, all obeying a Mohr–Coulomb failure criterion. It is worth nothing that, in the commercial software Strand7, neither non-linear orthotropic or softening materials are at user's disposal, therefore the assumptions made for the different masonry elements (elasto-plastic frictional materials) represent the most realistic choice that may be done in relation with the possible material models available in the code.

For masonry vaults, spandrels and the backfill, a pure Mohr–Coulomb failure criterion is adopted, with low cohesion and relatively high friction angle. No cut-off is considered in tensile stress. A perfect plastic behavior is assumed, within the classic hypotheses of plasticity theory (associated flow rule and infinite ductility of the material).

It is worth noting that the aforementioned assumptions about the non-linear behavior of the material may be restrictive with reference to masonry, which, at failure, exhibits an orthotropic behavior (as demonstrated by many authors, see for instance [28,29,32,33]), softening after the peak load and non-associativity. Nevertheless, such second approach is intrinsically more suited for the analysis of masonry structures when compared to a standard linear elastic computation, allowing a rough but quick preliminary estimation of the portions of the structure undergoing inelastic deformation, i.e. a prediction of crack patterns and failure mechanisms. In the Authors' opinion, most techniques of analysis are adequate, possibly for different applications, if combined with proper engineering justification [35]. Finally it must be underlined that, in case of massive structures with very low tensile strength, the post-peak behavior of cracked masonry has little influence on the global response and therefore no special attention was paid to the use of special software in order to include such an aspect.

2.2. FE homogenized non-linear code

The second approach adopted relies into FE computations performed by a noncommercial FE code [15,16,36], specifically crafted for the analysis in the non-linear range of 3D masonry structures. Within pushover simulations, barrel vault, external arches (when present) and spandrels, are modeled by means of orthotropic homogenized materials exhibiting softening and obtained with a homogenization approach similar to that proposed in [16], whereas infill is modeled by means of a Mohr–Coulomb material. It is interesting to notice that FE limit analysis simulations may be performed making use of the same software and the same discretization, simply assuming for the interfaces a rigid perfectly plastic behavior.

In the general case, i.e. with materials exhibiting softening, to solve the non-linear structural analysis problem, a Sequential Quadratic Programming (SQP) procedure within a discretization through rigid elements and non-linear quadrilateral interfaces, Fig. 3, again as in [15,16], is utilized. Each interface is supposed

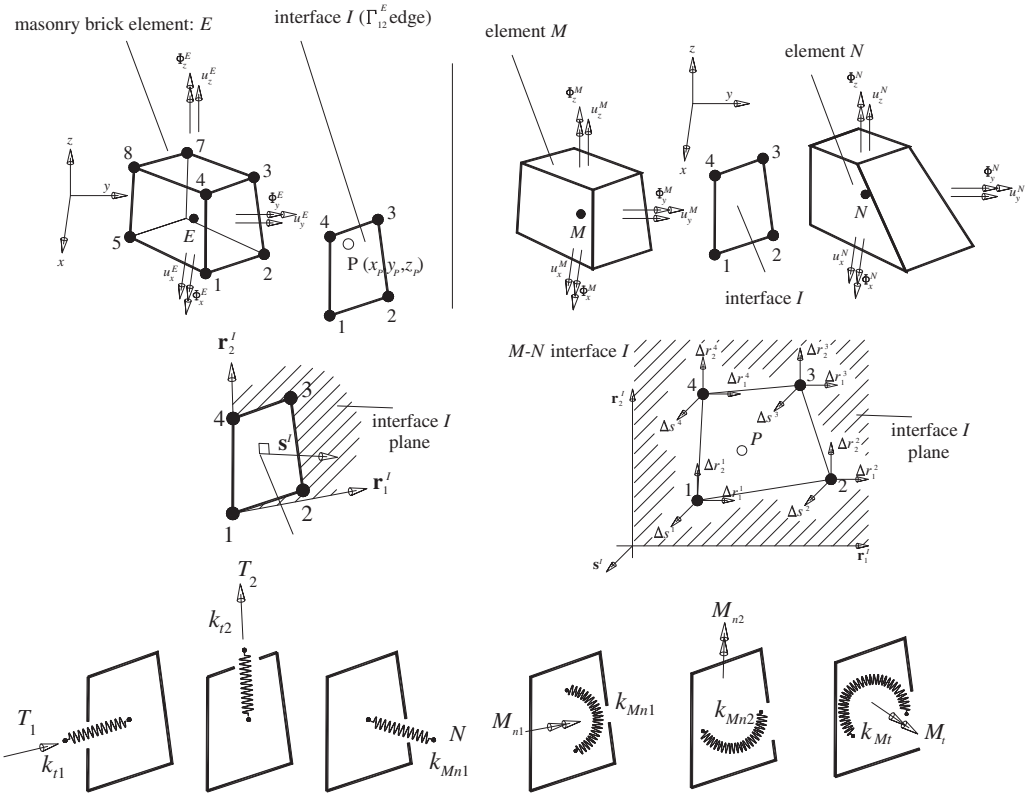

Fig. 3. Rigid infinitely resistant eight-noded parallelepiped element used for bridges 3D discretization and kinematics of interfaces between contiguous elements.

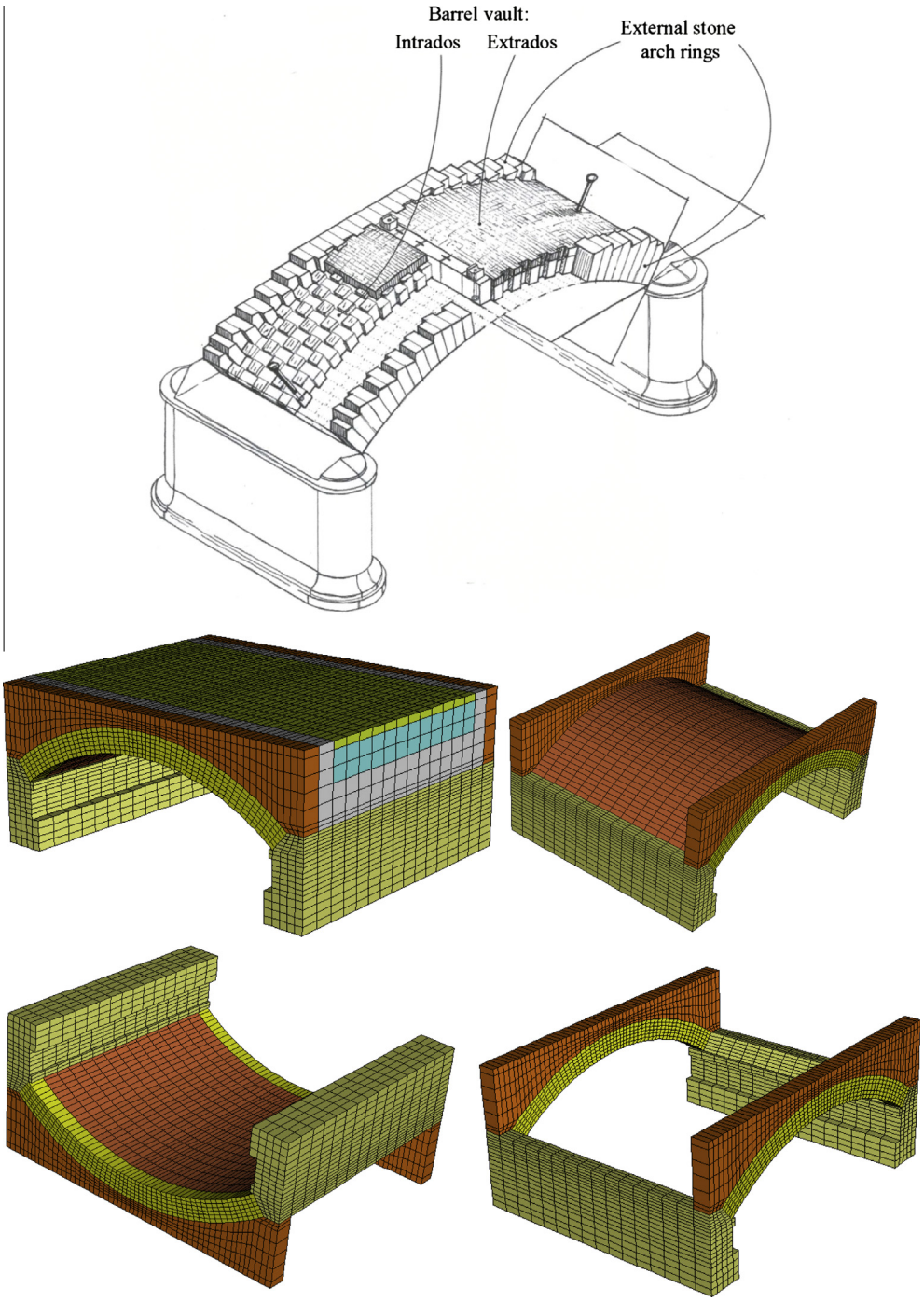

Fig. 4. Typical configuration of an arch barrel, adapted from Torre [37] and FE discretization of the Venice trans-lagoon bridge with identification of external stone arches (14,688 nodes and 12,224 bricks).

interconnected with adjoining elements by means of three non-linear displacement and three non-linear rotational springs.

In order to estimate the stress–strain non-linear behavior of both barrel vault and stone arches to be used at a structural level, a numerical homogenization procedure relying into a 3D FE discretization of the cell is adopted. The same code used at structural level is utilized to determine homogenized properties at cell level, with the only difference that within the unit cell the interfaces between contiguous elements are assumed isotropic.

For spandrels, since bricks are disposed in header bond and a FE discretization of the unit cell would be very demanding especially in the non-linear range, a simplified homogenization procedure with few plane-stress triangular elements and interfaces and already presented in [36] is adopted.

The non-linear uniaxial behavior of the displacement springs is thus deduced either by homogenization (FEM or simplified) or directly using the constitutive behavior of the isotropic material.

Kinematic variables for each rigid eight-noded element are thus represented by three centroid displacements (u_x^E,u_y^E,u_z^E) and three rotations around centroid $G(\Phi_x^E,\Phi_y^E,\Phi_z^E)$, see Fig. 3. The jumps of displacements on a point P of an interface is $[\mathbf{U}(P)] = \mathbf{U}_M^G - \mathbf{U}_N^G + \mathbf{R}_M(P-G_M) - \mathbf{R}_N(P-G_N)$, where $[\mathbf{U}(P)]$ is the displacement jump

between elements N and M in correspondence of point P, $\mathbf{U}_E^G$ is the E centroid displacement and $\mathbf{R}_E$ is the E rotation matrix.

Having defined a local frame of reference $\mathbf{r}_1^I - \mathbf{r}_2^I - \mathbf{s}^I$ for the interface between N and M elements (vertices corresponding to nodes P_1, P_2, P_3 and P_4, Fig. 3), we assume that it is characterized by two axes laying on the interface plane and mutually orthogonal, being the third axis perpendicular to the interface. Denoting with $\mathbf{R_e}$ the rotation matrix with respect to the global coordinate system, the jump of displacements may be written in the local system as $[\tilde{\mathbf{U}}(P)] = \mathbf{R_e}[\mathbf{U}(P)]$ where the superscript ~ indicates quantities evaluated in the local system.

Once the displacement jump in the local frame of reference is known, it is easily possible to evaluate both the displacement jump of the interface centroid G^I and the rotations of the interface.

To solve the discretized non-linear FE problem, under the hypotheses of elasto-plasticity, it has been shown that any

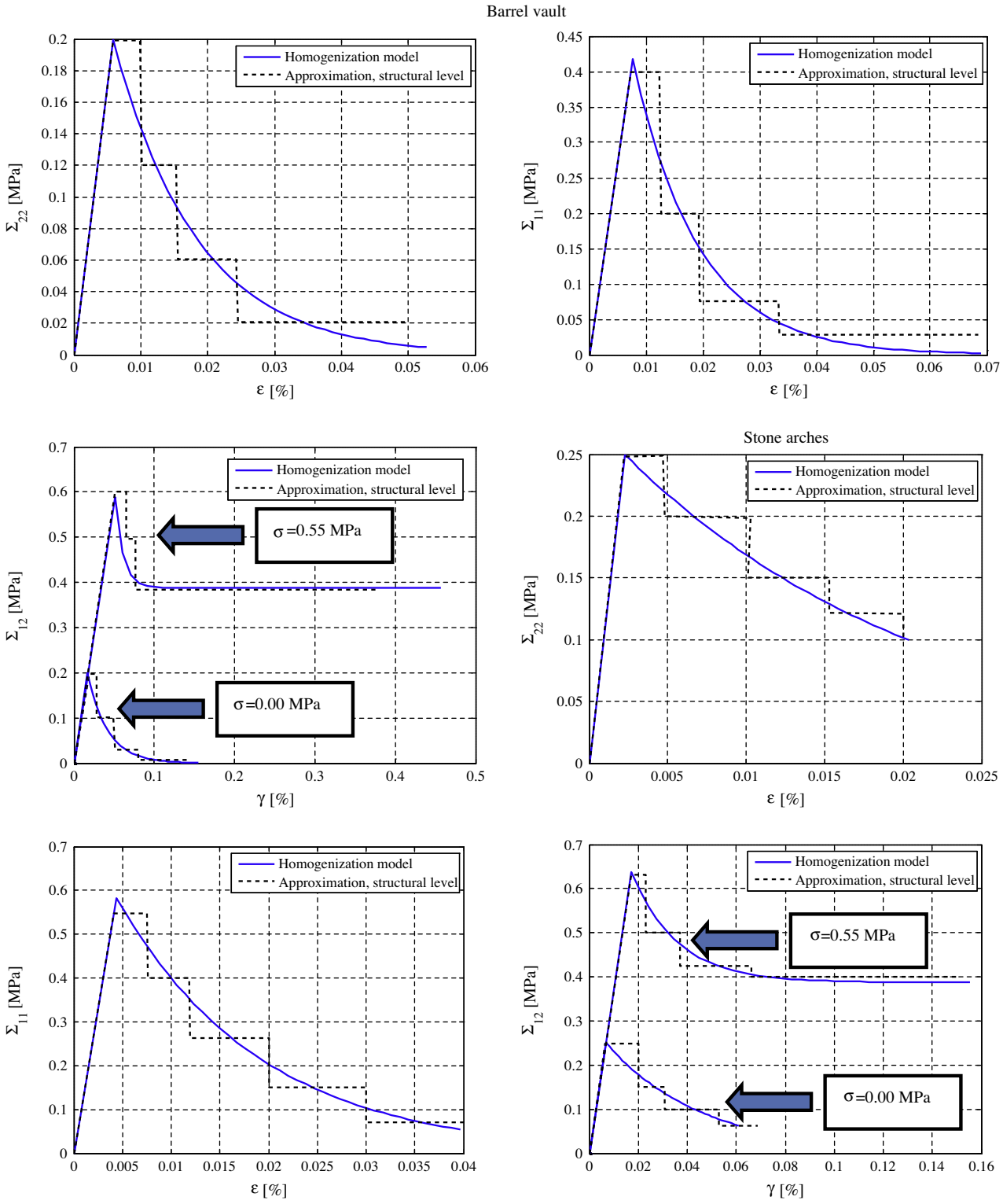

Fig. 5. Venice trans-lagoon bridge, stress–strain relationships used for barrel vault and stone arch.

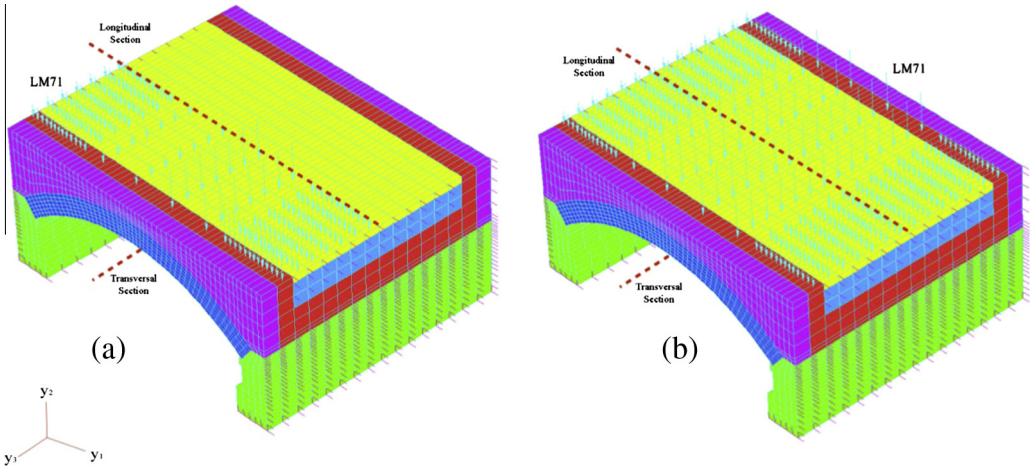

Fig. 6. The 3D model of a single arch with loads applied and transversal sections in which diagrams are taken.

structural problem may be solved incrementally by means of the constrained minimization of the total energy stored in the system, as follows:

$$\begin{cases} \max \left\{ -\frac{1}{2} \left(\boldsymbol{\lambda}^E\right)^T \mathbf{H}^E \boldsymbol{\lambda}^E + \left(\boldsymbol{\lambda}^E\right)^T \left(\mathbf{N}^E\right)^T \mathbf{D}^E \boldsymbol{\varepsilon}^E \right. \\ \textit{subject to} : \boldsymbol{\lambda}^E \geqslant \mathbf{0} \\ \boldsymbol{\varepsilon}_t^E = \boldsymbol{\varepsilon}^E + \boldsymbol{\varepsilon}_{pl}^E \\ \boldsymbol{\sigma}^E = \mathbf{D}^E \boldsymbol{\varepsilon}_{pl}^E \end{cases} \tag{1}$$

where $\mathbf{D}^E$ is the assembled elastic stiffness matrix, ε^E ($\boldsymbol{\varepsilon}_{pl}^E$) is the assembled elastic (plastic) part of the total strain vector $\boldsymbol{\varepsilon}_t^E$, $\mathbf{N}^E$ is the shape functions matrix of the used finite element, $\boldsymbol{\lambda}^E$ is the plastic multiplier vector, $\mathbf{H}^E$ is the hardening matrix and $\boldsymbol{\sigma}^E$ is the assembled stress vector.

When dealing with softening materials, it has been shown [16] that problem (1) may be again used iteratively, under the simplifying hypothesis that the stress–strain curves are approximated by means of a stepped function. Full numerical details of the proposed

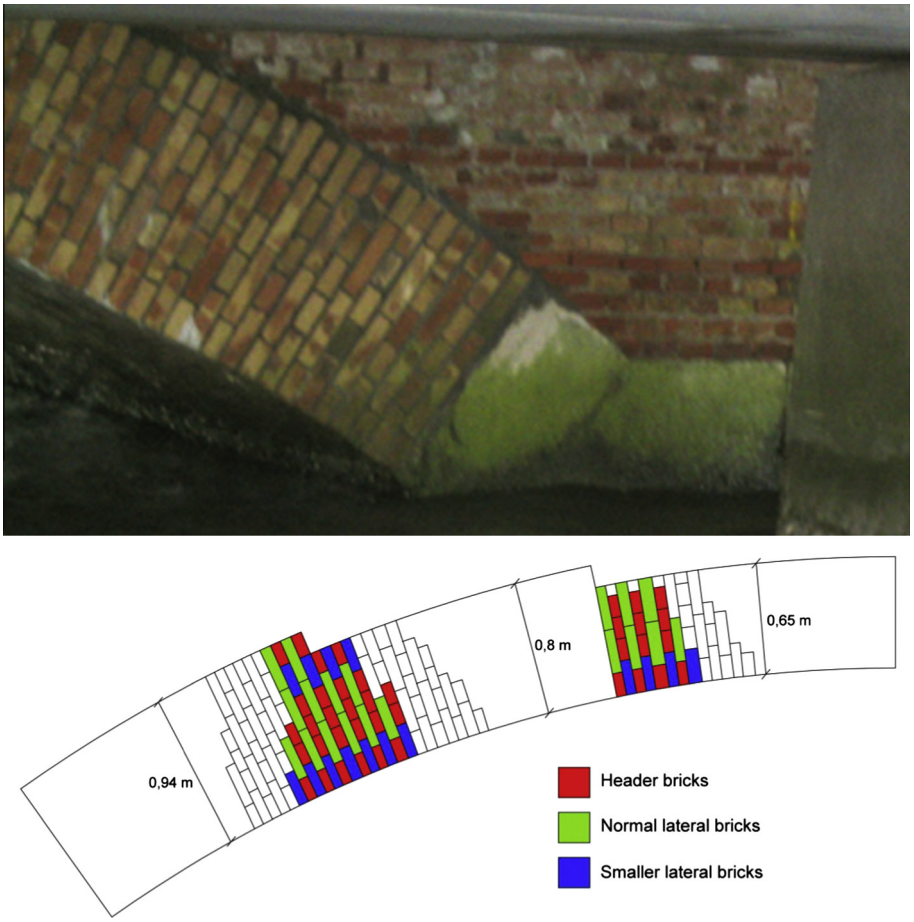

Fig. 7. The texture of masonry barrel vault.

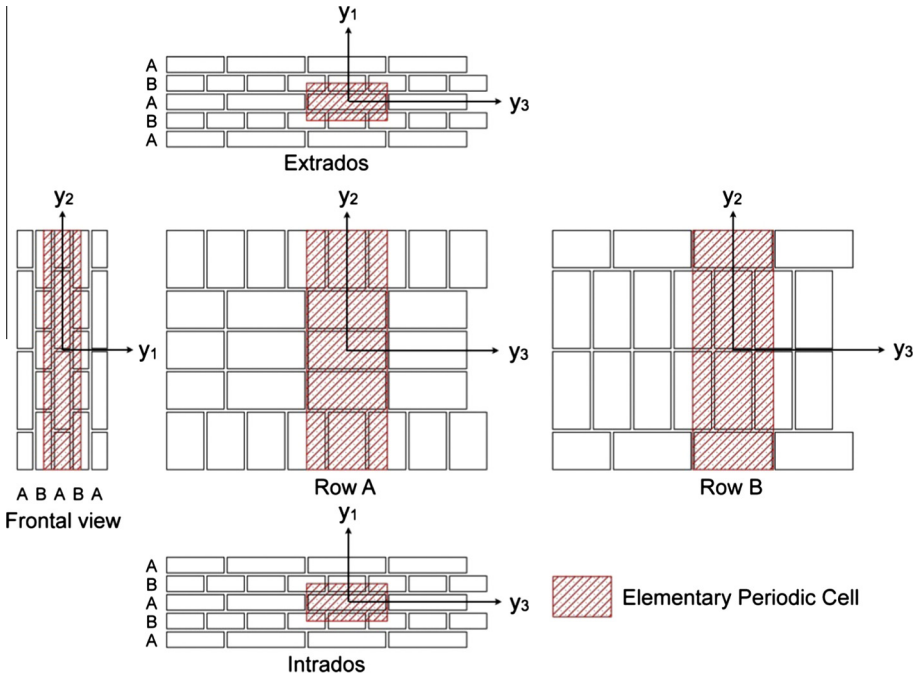

Fig. 8. The elementary cell for the homogenization of barrel vault.

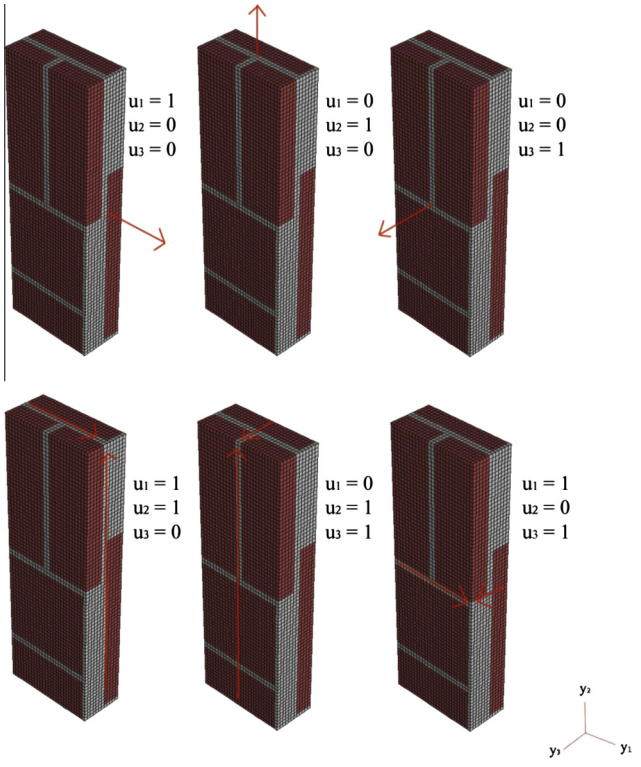

Fig. 9. FE homogenization model of the barrel vault elementary cell, with periodic boundary conditions applied.

approach may be found in [16], where the reader is referred for an insight. Here we only put in evidence that the resultant mechanical model is constituted by 6 elasto-plastic springs per interface, see Fig. 3 and [15]. Within each iteration, by means of the stepped function adopted as approximation for the real behavior, an elastic-perfectly plastic behavior for each spring is utilized, meaning that 12 plastic multipliers for each interface are needed (two for each spring, λ^+ and λ^-, corresponding to positive or negative kinematic variables). In this way, optimization variables entering into the QP problem are relatively small (12 plastic multipliers for each interface, 3 displacements and 3 rotations for each element).

Within the FE model adopted, it can be shown that problem (1) may be re-written as:

$$\begin{cases} \min \left\{ \frac{1}{2}[(\boldsymbol{\lambda}^+ - \boldsymbol{\lambda}^-)^T \mathbf{K}_{ep}(\boldsymbol{\lambda}^+ - \boldsymbol{\lambda}^-) + \mathbf{U}_{el}^T \mathbf{K}_{el} \mathbf{U}_{el}] - \mathbf{F}^T \mathbf{U}_{el} \right. \\ \textit{subject to} : \boldsymbol{\lambda}^+ \geqslant \mathbf{0}\ \boldsymbol{\lambda}^- \geqslant \mathbf{0} \end{cases} \tag{2}$$

Assuming that the structural model has n_{in} interfaces and n_{el} elements, symbols in Eq. (2) have the following meaning:

1. $\mathbf{K}_{el}$ is a $6n_{el} \times 6n_{el}$ assembled matrix, collecting elastic stiffness of each interface.
2. $\boldsymbol{\lambda}^+$ and $\boldsymbol{\lambda}^-$ are two $12n_{in}$ vectors of plastic multipliers, collecting plastic multipliers of each non-linear spring (e.g. flexion, shear, etc.).
3. $\mathbf{K}_{ep}$ is a $12n_{in} \times 12n_{in}$ assembled matrix built from diagonal matrices of hardening moduli of the interfaces.
4. $\mathbf{U}_{el}$ is a $6n_{el}$ vector collecting the displacements and rotations of the elements.
5. $\mathbf{F}$ is a $6n_{el}$ vector of external loads (forces and moments) applied on element centroids.

Typically, the independent variable vector is represented by element displacements $\mathbf{U}_{el}$ and plastic multiplier vectors $\boldsymbol{\lambda}^+$ and $\boldsymbol{\lambda}^-$.

To deal with softening, an iterative procedure based on QP is adopted, as shown extensively in [16], where the reader is referred to for details. QP problem (2) is solved in terms of displacement

Table 1
Elastic properties adopted for the homogenization of the barrel vault.

	Young's modulus (MPa)	Poisson's ratio	Density (kg/m^3)
Bricks	$E^B = 5000$	$\nu^B = 0.2$	$\rho^B = 1800$
Mortar	$E^M = 1000$	$\nu^M = 0.2$	$\rho^M = 1800$

Table 2
Mechanical properties (linear and non-linear) adopted in the numerical simulations with the non-commercial code, structural level.

	Barrel vault				
	Mortar	Blocks	Backfill		
E	1000	5000	1400	(MPa)	Young modulus
G	450	2200	500	(MPa)	Shear modulus
c	$1.0f_t$		0.12–0.08–0.04	(MPa)	Cohesion
f_t	0.20		$c/\tan\Phi$	(MPa)	Tensile strength
Φ	36		30–20	(°)	Friction angle
G_f^I	0.003		Elastic-perfectly plastic	(N/mm)	Mode I fracture energy
G_f^{II}	$2G_f^I$		Elastic-perfectly plastic	(N/mm)	Mode II fracture energy
	Stone arches		Spandrels		
	Mortar	Blocks			
E	1000	13,000	2800	(MPa)	Young modulus
G	450	5600	1200	(MPa)	Shear modulus
c	$1.0\ f_t$		$1.4f_t$	(MPa)	Cohesion
f_t	0.25		0.18	(MPa)	Tensile strength
Φ	36		36	(°)	Friction angle
G_f^I	0.03		0.04	(N/mm)	Mode I fracture energy
G_f^{II}	$2\ G_f^I$		$2G_f^I$	(N/mm)	Mode II fracture energy

Table 3
Homogenized elastic properties of the barrel vault.

E_{11}	E_{22}	E_{33}
Young's modulus (MPa)		
3480	3592	2861
G_{12}	G_{23}	G_{31}
Shear Modulus (MPa)		
1340	1100	1120
ν_{12}	ν_{23}	ν_{31}
Poisson's ratio		
0.18	0.194	0.158

and plastic multipliers step increments. The initial solution of the problem is always represented by the solution at the previous step.

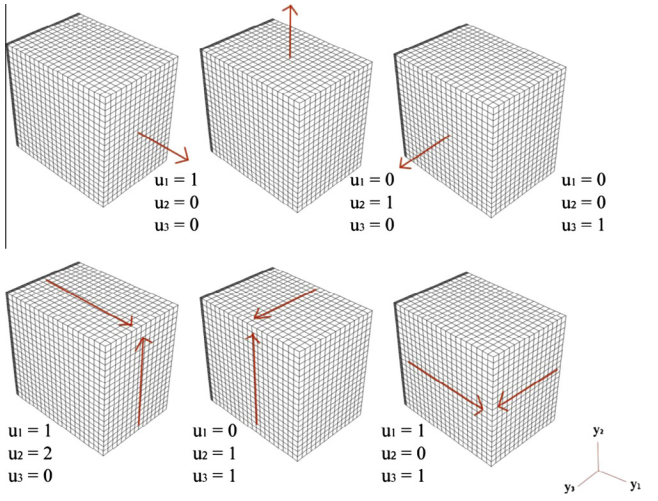

Fig. 10. Elementary cell and FE model with periodic boundary conditions applied, stone arch.

3. Application to the trans-lagoon Venice bridge

3.1. Historical description of bridge

The trans-lagoon Venice bridge was built in 1846. During its life, it was subjected to many interventions of restoration and modification of the original project, and it is now the result of more than 150 years of history [25,37,38]. The bridge, see Figs. 2 and 4, relies into 222 arches, divided in 6 modules of 37 arches, named "stadii", separated from the close ones by artificial islands. Each module is divided in 7 sequences of 5 arches, except the central one of 7 arches: between each sequence there is a big pier ("pila–spalla") in order to prevent a global collapse due to the fall down of a single arch. For this reason the bridge can be reasonably considered as a sum of minor bridges. Fig. 2 represents one stadium: it is possible to notice the sequences of arches and the difference between the artificial islands (A), the big piers (B and C) and the normal piers (numbered or P).

Each arch has a span of 10 m and a rise of 1.73 m, with a ratio S/R equal to 1:1.58. The vault has a curvature radius of 8.80 m at intrados and a transversal length of 9 m. The thickness changes: 0.65 m at the crown, 0.80 m in the half of middle span, 0.94 m at the abutments. Abutments and piers are made of Istrian stones. Foundations are realized with the typical technology of historical Venetian buildings: wooden larch piles fixed in the lagoon bed.

Table 4
Elastic properties adopted for the homogenization of the stone arch.

	Young's modulus (MPa)	Poisson's ratios	Density (kg/m^3)
Stone	$E^S = 10{,}000$	$\nu^S = 0.2$	$\rho^S = 2700$
Mortar	$E^M = 1000$	$\nu^M = 0.2$	$\rho^M = 1800$

The arch barrel and the spandrel walls are made by Venetian bricks. Backfill is made by heterogeneous incoherent materials.

3.2. Discretization adopted and load cases considered

The 3D FE discretization adopted for the numerical analyses within all models is schematically depicted in Fig. 4. The discretization is obtained by means of a suitable extrusion of a 2D model, taking into account the actual disposition of the different structural elements along the thickness (spandrels, external arch rings, backfill and masonry vault) basing on a detailed analysis of historical transversal sections available to the authors [26], see Fig. 2. The 2D model is previously discretized on the base of both direct

Table 5
Homogenized elastic properties of the stone arch.

E_{11}	E_{22}	E_{33}
Young's modulus (MPa)		
8335	9823	9823
G_{12}	G_{23}	G_{31}
Shear modulus (MPa)		
3416	4075	3416
ν_{12}	ν_{23}	ν_{31}
Poisson's ratio		
0.17	0.19	0.20

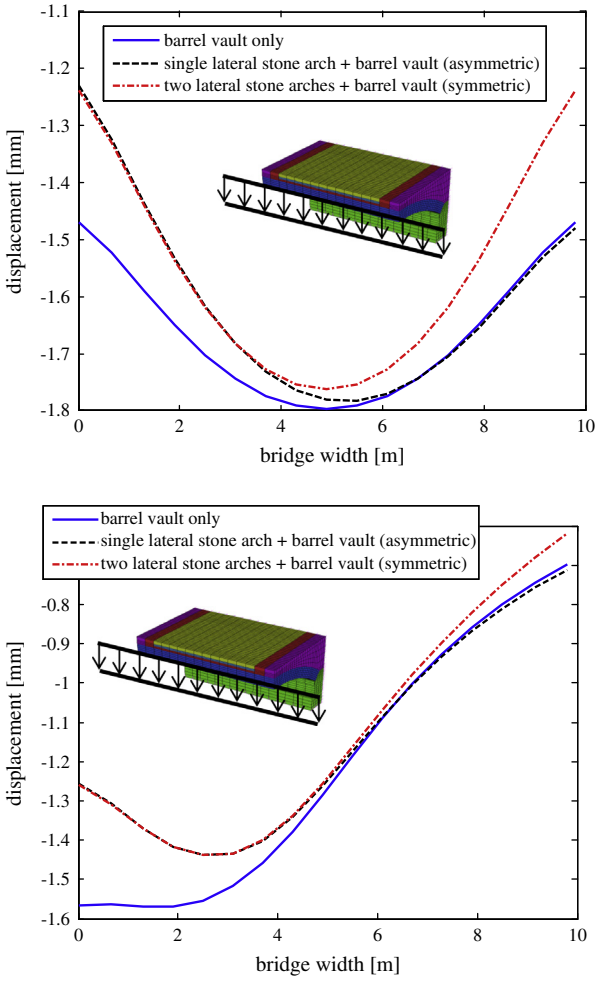

Fig. 11. Vertical displacements at intrados of crown. Top: LM71 on both rails. Bottom: LM71 on single rail.

survey of the authors (conventional topographic and photogrammetric data) and available historical documentation.

The mesh is quite refined and regular and relies in parallelepiped eight-nodes elements with low distortion ratio and with distinct properties of each meaningful structural element (barrel vault, piers, rings, spandrels, backfill, infill and railway ballast). For the case under study, the barrel vault is completely made by brick masonry. However, several masonry arch railway bridges built in the same period, were typically conceived with two external arch rings made by stone voussoirs, with the internal part made by brick masonry [37], see Fig. 4. In this latter case, it has been sometimes experienced a larger thickness of the external rings

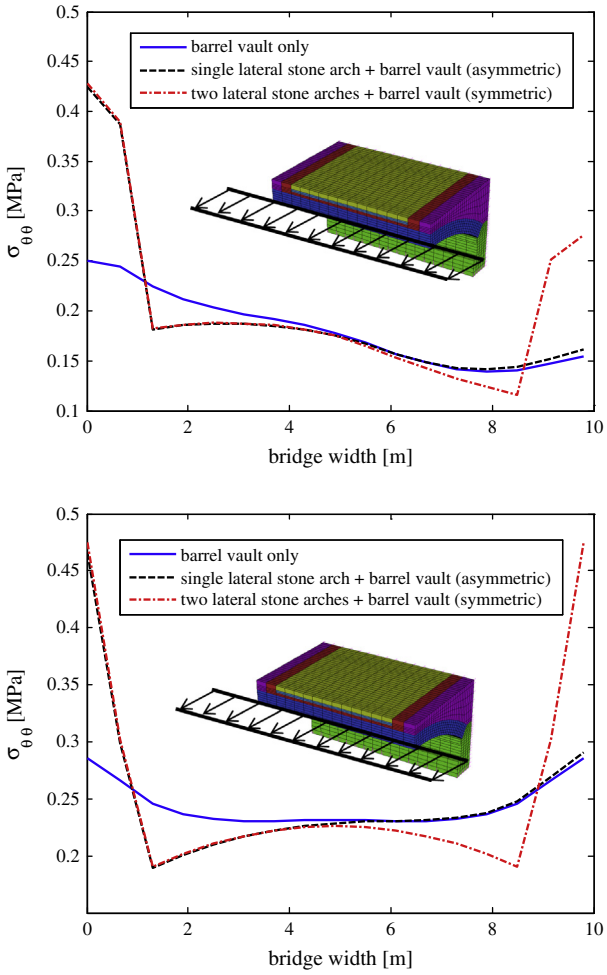

Fig. 12. Horizontal stresses at intrados of crown. Top: LM71 on both rails. Bottom: LM71 on single rail.

when compared with that of the central barrel vault. In this work, apart the actual configuration of the Venice trans-lagoon bridge, the hypothesis of the existence of two external stone arch rings has been made: the aim is to investigate the influence of the rings on the structural behavior of the bridge.

Considering the consistent and growing rail traffic that at present the bridge is called to carry, an evaluation of its behavior under service and ultimate (collapse) loads may provide interesting information respectively on the assessment of functionality and load bearing capacity, with the aim of ensuring its conservation or to improve/refurbish its structural performance.

Having this target in mind, the static analyses are conducted in both the linear and non-linear field. In particular, the following FE simulations are conducted:

(1) Linear static analyses, suited to investigate the behavior under service loads. In this case, only the commercial software is utilized. Different hypotheses on the vaults, supposed exclusively constituted by a thick brick masonry layer or by the vault and two external stone stiffening arch rings, see Fig. 4, are made. Elastic properties of both the vault and the arch rings are obtained by standard linear elastic FE homogenization, see [29,32,39–41]. Two different load cases are investigated, the first simulating the passage of a train on a single track and the latter on both tracks. The entity of the traffic loads are provided by Italian Railway regulations [42].

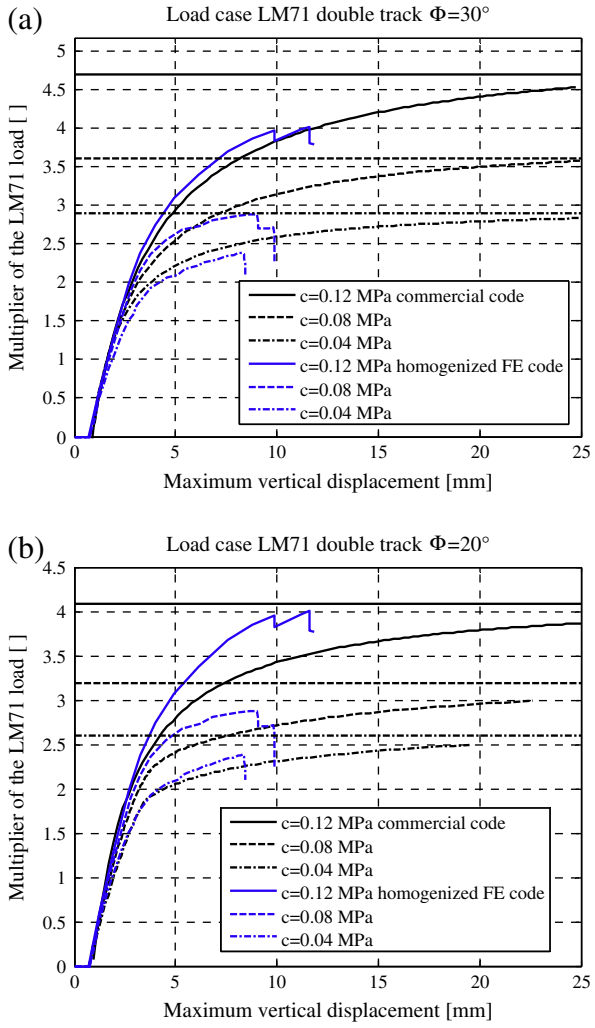

Fig. 13. LM71 load on both tracks without stone arches. Load displacement curves at different values of infill cohesion at two different friction angles: (a) 30°, and (b) 20°.

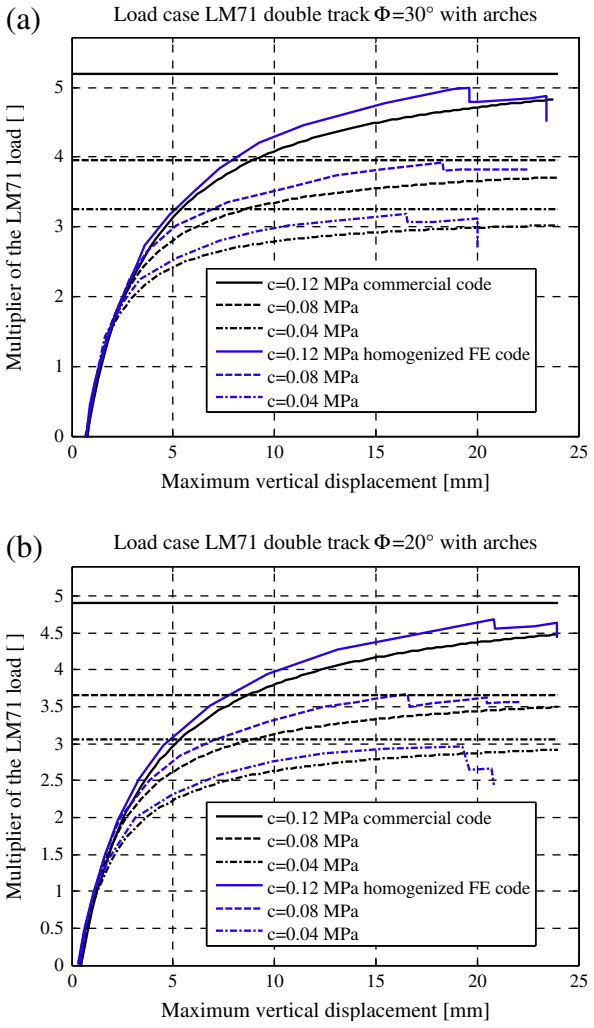

Fig. 14. LM71 load on both tracks with stone arches. Load displacement curves at different values of infill cohesion at two different friction angles: (a) 30°, and (b) 20°.

In particular, Italian Railways require to apply two different typologies of loads labeled as LM71 and SW2, differing for both the entity and typology of loads (pressures and concentrated forces), position and application length. For the specific case at hand, it is found that LM71 is less conservative when applied symmetrically with respect to the middle span of the structure. Usually, it is found that such structures, despite quite dated, may resist well against the passage of heavy trains. It is however important to have an insight into the entity of displacements induced by a passage of a train and, eventually, investigate with more attention the behavior under repeated load condition.

(2) Non-linear static analyses, suited to investigate the behavior of the structure beyond elasticity, under external loads increased up to the activation of a failure mechanism. In this context, two different typologies of analysis are conducted, namely pushover (which relies into an incremental procedure with non-linear materials) and limit analysis. When dealing with limit analysis the materials are assumed rigid-plastic and the procedure allows obtaining the active failure mechanisms and the associated collapse load, without providing any indication on displacements near failure. This second set of simulations is performed using both the commercial and non-commercial software. In both cases, the interaction between the barrel vault and the backfill is accounted for. When the commercial code is used, as already pointed out, isotropic materials are adopted [34,26]. In addition, elastic-perfectly plastic materials obeying an associated flow rule under a classic Mohr–Coulomb failure criterion are assumed. When dealing with the non-commercial software, softening orthotropic materials are assumed [15,16]. Limit analysis simulations are obtained excluding softening from the computations, with the same code used for the non-linear analyses [33]. In presence of softening, the stress–strain relationships for the different materials constituting the bridge and depicted in Fig. 5 are utilized. Within limit analysis, peak values in Fig. 5 are assumed. In this latter case, while the less realistic hypothesis of infinite ductility of the materials is assumed instead of a more consistent decrease of the strength at high deformations, it is expected that softening in tension and shear have little effect on the global pushover curves, especially within the range of small-moderate displacements. The loads considered in the non-linear static analyses belong to two categories: the first is a vertical load simulating the passage of a train, increased up to failure of the structure, whereas the second is a settlement of one of the piers, again increased up to collapse. When dealing with the first typology, the amount and typology of loads applied on the models are provided by technical

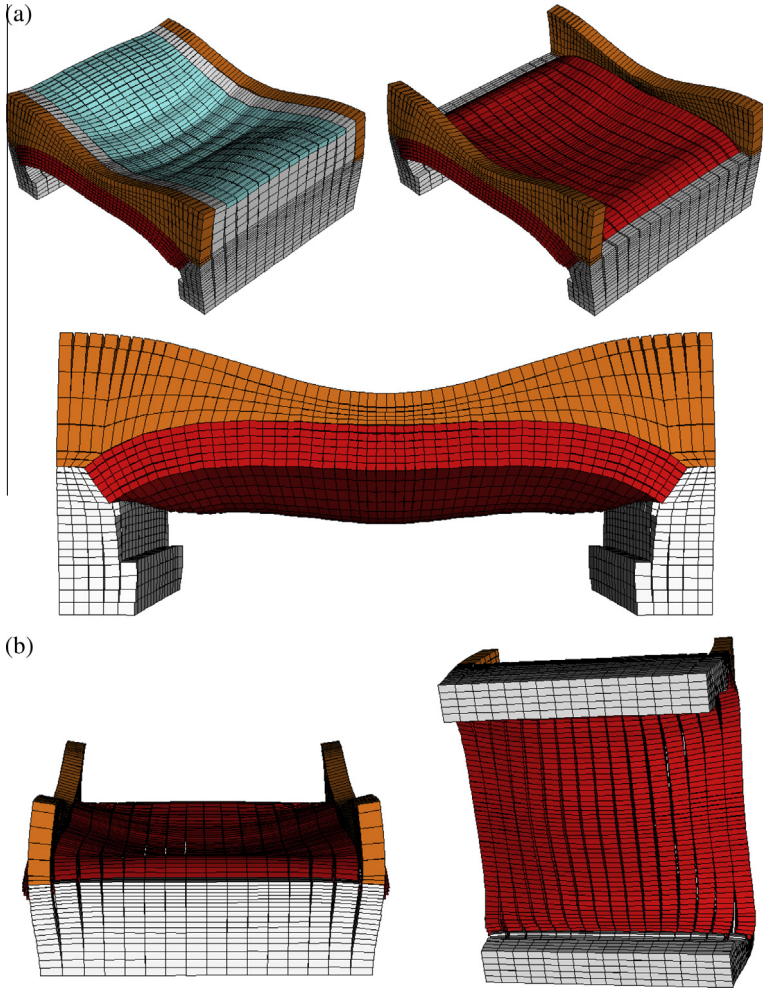

Fig. 15. LM71 load on both tracks. Deformed shape obtained with the non-commercial FE code. (a) Perspective view. (b) Lateral, front and bottom views.

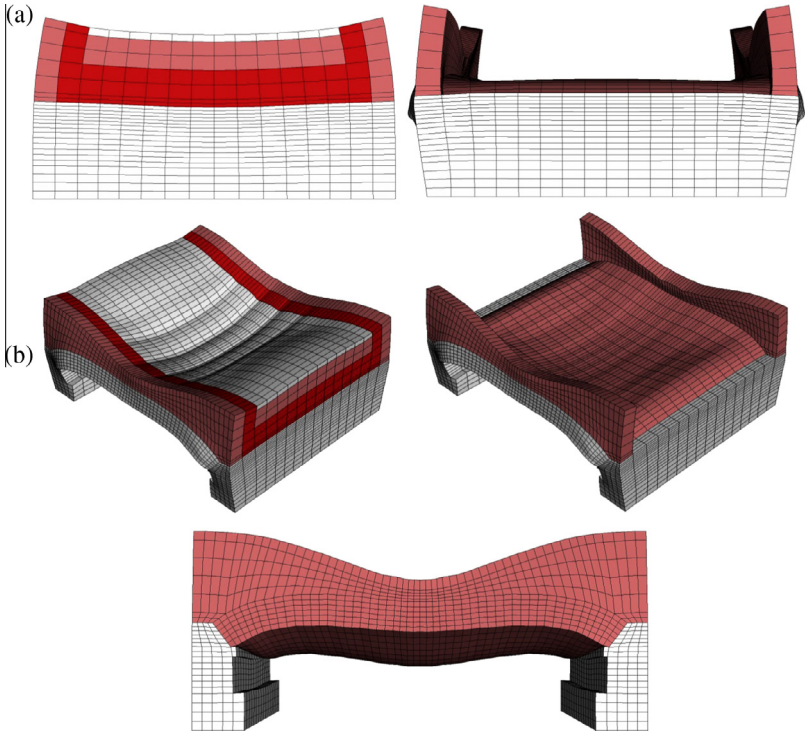

Fig. 16. LM71 load on both tracks. Deformed shape obtained with the commercial FE code. (a) Front. (b) Perspective and lateral views.

Italian regulation [42]. In particular, as already pointed out, any bridge should be loaded by the two train load typologies provided by regulation, called LM71 and SW2. LM71 is a load applied on the whole span, whereas SW2 is a single span load typology. LM71 seems associated generally to higher internal stresses and deflections on the bridge and hence the discussion is here limited to LM71. The loads have been applied in order to evaluate both the longitudinal and the transversal behavior of the bridge. When dealing with the longitudinal behavior, two parallel LM71 loads have been assumed to act symmetrically on the bridge, whereas the transversal effect has been investigated with a single LM71 load placed eccentrically on a single track, as illustrated in Fig. 6. When dealing with the foundation settlement, an increasing vertical displacement is imposed at the base of one of the piers. No limit analysis predictions can be obtained in this case, as a consequence of its well-known inability to provide any information on displacements at failure. Such load case appears quite realistic, especially for the Venice lagoon, where the soil mechanical properties may both vary quickly from point to point and are generally very low.

3.3. Homogenization of barrel vault and stone arches by means of a 3D FE discretization of the elementary cell

A preliminary homogenization in the elastic and non-linear case, Fig. 5, to evaluate the stiffness and non-linear stress–strain behavior of masonry barrel vault and stone arches at a structural level is performed. At the micro-scale, an elementary cell (also called Representative Element of Volume or REV), which provides all the geometrical and mechanical characteristics needed to completely describe the whole masonry wall by its repetition, is identified and suitably meshed with the same parallelepiped rigid and infinitely resistant elements interconnected by inelastic interfaces used at a structural level, see previous Section.

3.3.1. Homogenization of the barrel vault

The barrel vault under consideration and the REV used in the numerical simulations are depicted in Figs. 7 and 8 respectively. A standard FE homogenization procedure, see [28,29,32,39–41] for theoretical details, is performed to estimate mechanical properties (both elastic moduli and stress–strain curves) to be used at a structural level.

The discretization adopted within a well-established displacement based procedure, with unitary displacements applied in

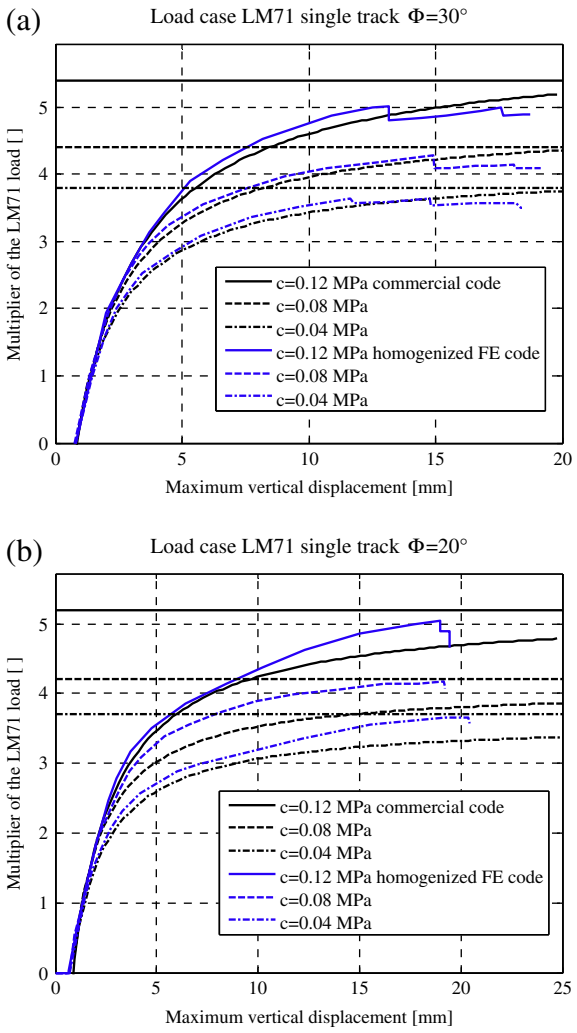

Fig. 17. LM71 load on single track without stone arches. Load displacement curves at different values of infill cohesion at two different friction angles: (a) 30°, and (b) 20°.

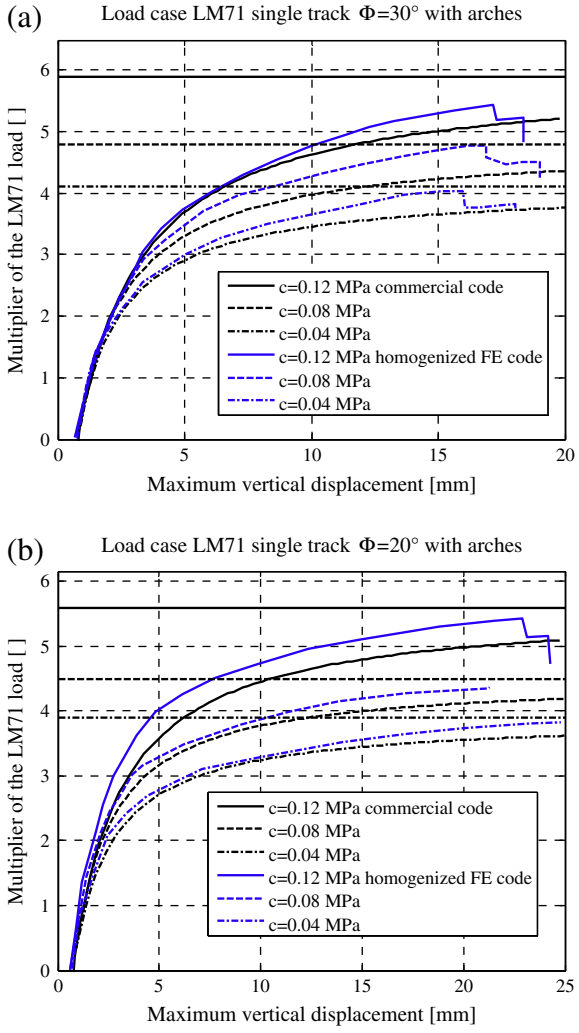

Fig. 18. LM71 load on single track with stone arches. Load displacement curves at different values of infill cohesion at two different friction angles: (a) 30°, and (b) 20°.

linear elasticity in the various cases and constraints are depicted in Fig. 9.

The REV has been identified on the base of the real arrangement of the bricks. However, some hypotheses have been formulated on the base of the visible bricks pattern – as shown in Fig. 7 – and on the base of drawings of the original project, due to the impossibility of a direct view of the internal bricks. Considering the arrangement of blocks along the arch ring, two rows of bricks have been identified, as shown in Fig. 7. The barrel vault has been considered with a constant thickness of 800 mm for the sake of simplicity in the structural model, however in reality it has a lower thickness at crown and a higher thickness at abutments. The bricks have the typical dimensions of historical Venetian bricks, equal to $250 \times 120 \times 50$ mm^3. The thickness of mortar joints is about equal to 10 mm. Both bricks and mortar have been modeled as isotropic materials. The mechanical properties adopted for the model of the REV are reported in Table 1 (elastic properties) and in Table 2 (inelastic properties).

Considering the small dimensions of the REV when compared to the whole barrel vault, the problem has been geometrically linearized, reasonably assuming a flat REV.

The elastic properties obtained by homogenization are reported in Table 3, whereas the inelastic axial behavior (along a horizontal and vertical direction) and shear to be used within the non-linear approach are depicted in Fig. 5. In Fig. 5, it is also reported the stepped approximation used in the non-commercial FE code [15,16], needed to perform Sequential Quadratic Programming computations.

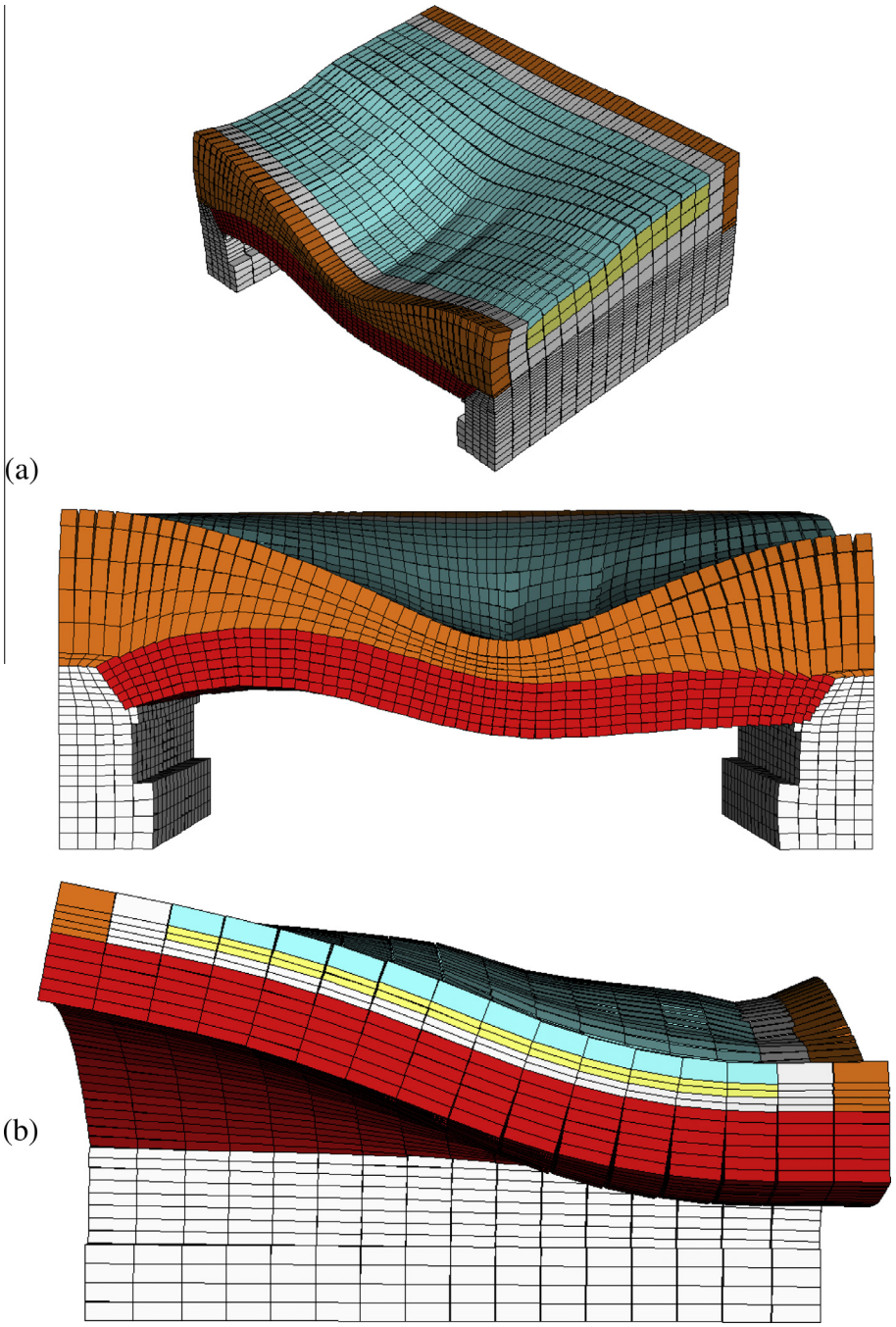

Fig. 19. LM71 load on single track. Deformed shape obtained with the non-commercial FE code. (a) Perspective and lateral views. (b) Front view.

3.3.2. Homogenization of the stone arch

The same homogenization procedure has been applied to a hypothetic texture of a stone arch, with REV as in Fig. 10. The thickness of the arch rings has been assumed constant and equal to the thickness of the barrel vault, therefore equal to 800 mm. The arch rings are assumed made of blocks having dimensions equal to $800 \times 400 \times 300\ mm^3$. Mortar joints thickness is assumed equal to 5 mm. Both bricks and mortar have been modeled as isotropic materials by means of brick elements. Elastic mechanical properties adopted for the constituent materials of the REV are reported in Table 4, whereas inelastic parameters of stones and mortar are summarized in Table 2.

Also in this case, as previously described, considering the small dimensions of the REV when compared to the entire arch ring, the REV has been considered flat. The elastic properties obtained through homogenization are summarized in Table 5, whereas its axial and shear inelastic behavior is depicted in Fig. 5.

4. Results of the numerical analyses under conventional train loads

The results of a number of numerical simulations performed in the linear and non-linear range under conventional train loads acting, and performed by means of both the commercial and non-commercial software, are here presented and critically compared.

Numerical simulations comprise linear elastic analyses under service loads, non-linear pushover analyses with two different load conditions up to failure, limit analyses and pile settlement simulations, with displacements increased up to failure of the structure. 3D effects and role played by the backfill are critically analyzed in light of the numerical results obtained with the three approaches comparatively used.

4.1. Linear analyses: serviceability conditions

Preliminarily, a parametric linear static analysis has been performed to evaluate the sensitivity of the global behavior of the bridge to the presence or absence of the stone arch rings under service condition. Among all the analyses performed, only the most meaningful results are here reported. A synopsis of the numerical data obtained is represented in Figs. 11 and 12.

In particular, Fig. 11 shows the vertical displacements of the intrados nodes at the top of the barrel vault, whereas in Fig. 12 the stresses along the horizontal direction (longitudinal direction of the bridge) on the same nodes are depicted.

In the diagrams, continuous lines represent the barrel vault completely made of bricks, dashed lines represent the bridge with one external stone arch ring and dash-dotted lines the bridge with two symmetric external stone arches.

As can be noted, Fig. 11 shows clearly that vertical displacements at intrados of crown of the model with the two external stone arch rings are sensibly smaller then the displacements of the model representing the actual configuration. Fig. 12 shows that there is a transmission of stresses between the barrel vault and the external stone arch rings, with a consequent reduction of stresses in the barrel vault. This effect is reduced near the center, due to the considerable transversal thickness of the structure, which is of the same order of magnitude of bridge span.

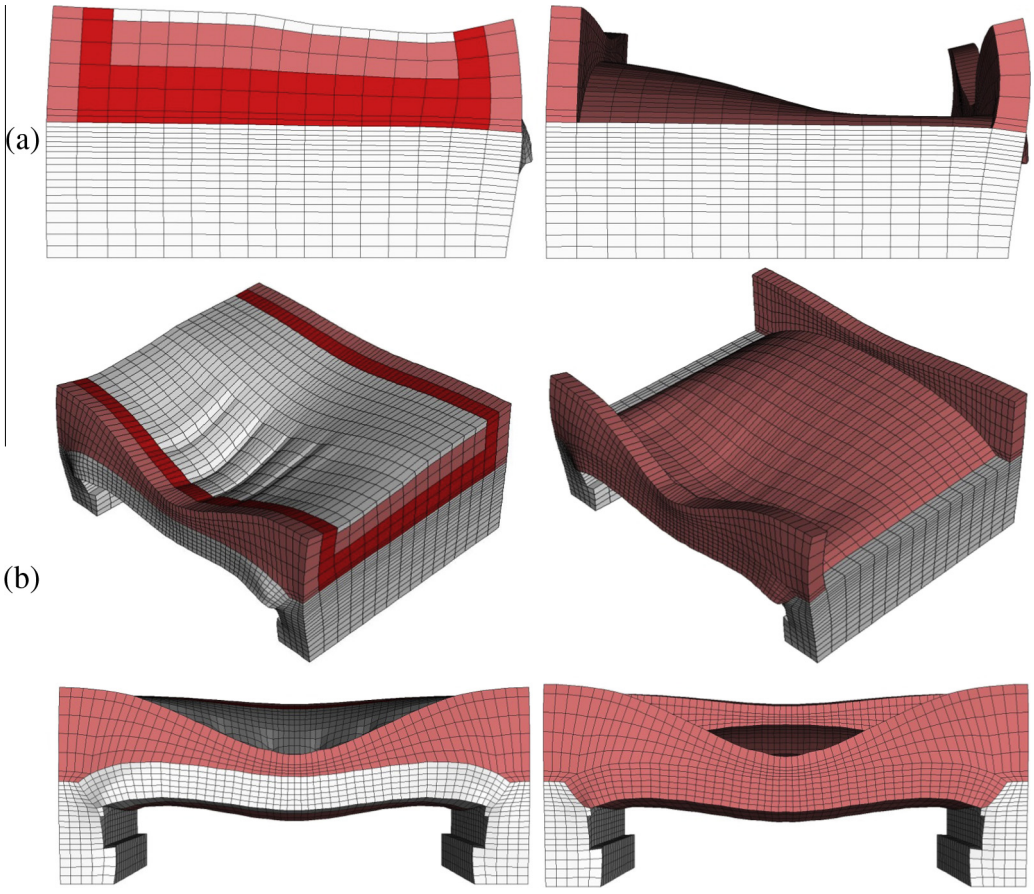

Fig. 20. LM71 load on single track. Deformed shape obtained with the commercial FE code. (a) Front and (b) Perspective and lateral views.

4.2. Nonlinear analyses: effect of backfill and spandrels

The contribution of the backfill in stabilizing a bridge has been well known from many years. For instance, in the 40's of the last century, some authors noticed a change of the line of thrust caused by the backfill in arch bridges [43], but the importance of backfill became clearer in the 60's, when some researchers shown a higher load-bearing capacity due to backfill contribution [44,45].

The presence of a solid joint may allow the development of a flat arch inside the backfill. This phenomenon can change the span of the arch, as demonstrated for instance by the collapse of Traversa Railway Bridge in the Italian railway between Torino and Genova [46]. An evaluation of the increase in the load bearing capacity due to backfill can be found in Smith [47], whereas the role of the other structural elements has been studied by Molins and Roca [48], which showed an increase of the failure load when modeling not only the arch itself but also the other elements. Similar numerical analyses with comparable results have been performed by Cavicchi and Gambarotta [11–14], who studied the influence of the backfill on two literature bridges with a 2D upper bound approach.

The numerical simulations here performed with both Strand7 [34] and the non-commercial code [15,16] are conducted performing several pushover analyses assuming for the backfill a Mohr–Coulomb failure criterion with elastic-perfectly plastic behavior, and a sensitivity analysis is performed changing cohesion and friction angle in a realistic range. In particular, three values of cohesion for the backfill are investigated equal to 0.04, 0.08 and 0.12 MPa, associated with two values of the friction angle, equal to 30° and 20°. According to literature data, the most realistic mechanical properties for an existing backfill in a bridge are a very low cohesion (well approximated by the lower value here investigated) and a moderately high value of friction angle, typically around 30–35°.

Pushover analyses are conducted with either FE codes increasing up to failure the train load LM71, in presence and absence of lateral stone arches and assuming both configurations for the external load, i.e. the symmetric and unsymmetrical one, simulating the presence of trains on whole bridge or on a single track respectively.

A huge amount of numerical simulations has been performed, namely 24 pushover analyses for both codes utilized, i.e. with and without reinforcing stone arches, two load cases, three different cohesions of the backfill and two different friction angles.

In addition, FE limit analyses have been repeated on the same FE discretization with a limit analysis code previously developed by one of the authors [49], in order to have a precise prediction of the entity of the loads associated to the collapse of the structure, without the need to perform computationally expensive incremental simulations. In any case, it is worth noting that software

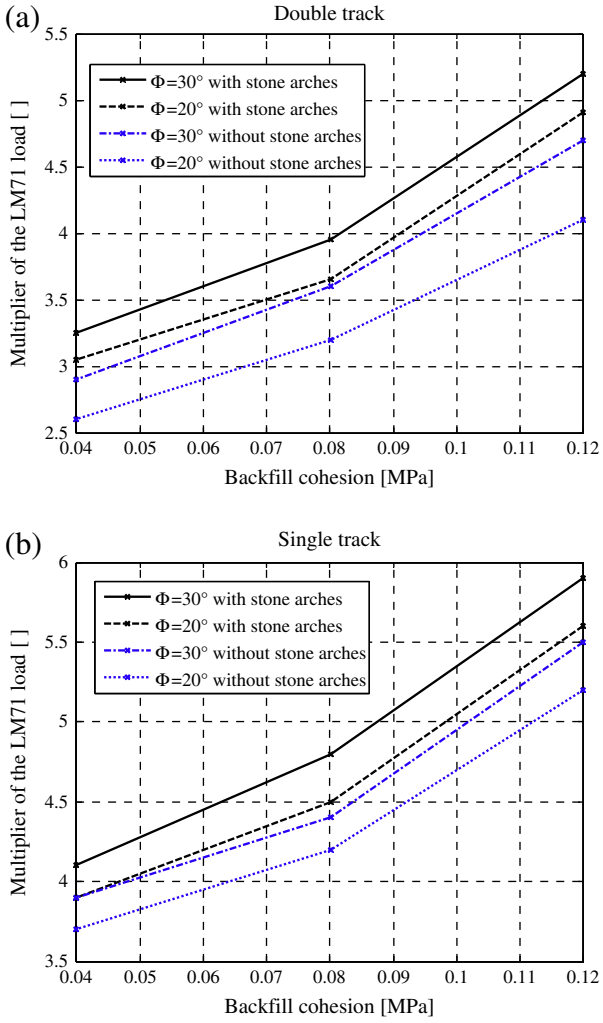

Fig. 21. Synopsis of failure loads obtained with limit analysis. (a) LM71 load on both tracks. (b) LM71 load on single track.

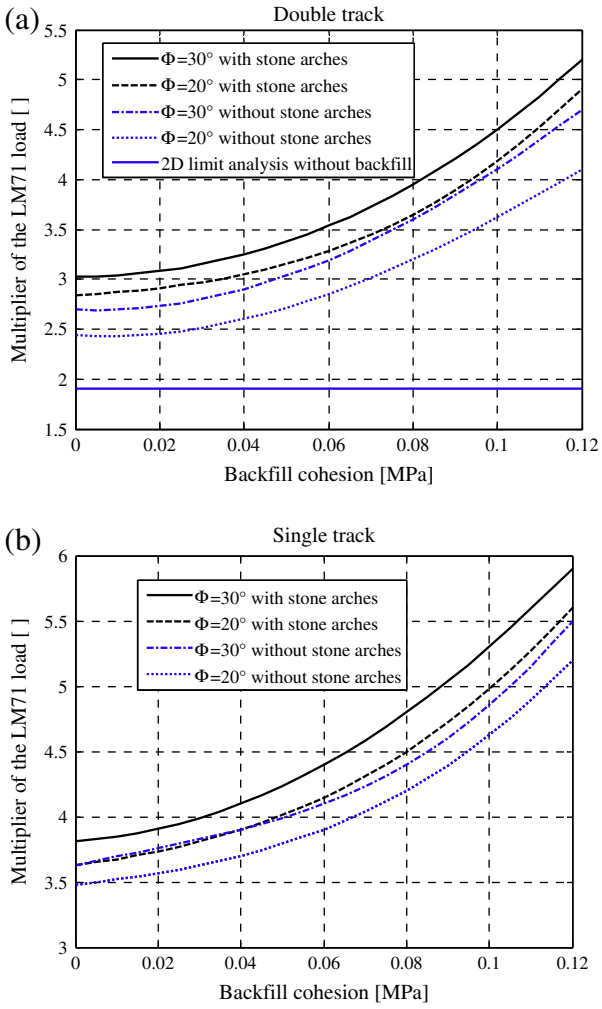

Fig. 22. Data extrapolation for backfill with vanishing cohesion and comparison with results obtained with a 2D approach in absence of backfill (double track).

available in [15,16] is capable of providing the same final results when elastic-perfectly plastic materials are assumed.

Pushover curves and failure loads so obtained are shown from Fig. 13 to Fig. 20 for all the cases investigated, along with deformed shapes at collapse provided by both the commercial and non-commercial FE software.

From an overall and comparative analysis of simulations results, the following considerations may be drawn:

(1) The role played by the backfill in increasing the load bearing capacity is quite evident from results and once again its stabilizing effect against vertical loads is confirmed, as already pointed out by classic literature [11–13].
(2) The ultimate loads obtained for the three values of cohesion and the two values of friction angle inspected for the backfill are comparatively represented in Fig. 21. It is interesting to notice that ultimate loads of the bridge associated to a backfill with no cohesion may be easily deduced from Fig. 21 after proper data extrapolation, see Fig. 22. Collapse loads obtained in absence of cohesion reasonably represent the lower bound values expected in practice and should be compared with collapse loads obtained in absence of backfill to estimate the beneficial role played by the backfill in increasing the load bearing capacity of such structures.
(3) In Fig. 22-a, a comparison between failure loads obtained in absence and presence of backfill is shown for the symmetric case and absence of external stone arches. Only in this latter case, indeed, the utilization of 2D limit analysis approaches, as for instance Ring [6], is possible. As can be noted, even in presence of backfill with zero cohesion and small friction angle, the increase of the load bearing capacity with respect to the case without backfill is greater than 50%.
(4) Friction angle has a clearly evident role on the increase of the load bearing capacity of the structure, for all the cases investigated and especially in presence of vanishing cohesion of the backfill and without lateral stone arches. The presence of the stone arches, indeed, increases the load bearing capacity of the structure, making the stabilizing role of the backfill less evident.
(5) The introduction of the lateral stone arches is quite beneficial, since it is associated clearly to an increase of both stiffness and strength of the structure. Such feature is well reproduced by all models.
(6) Orthotropy of the barrel vault and the spandrels has little influence on the global behavior of the structure, as clearly shown by the small discrepancies of the pushover curves provided by the commercial code (isotropic materials) and the non-commercial software with rigid elements and non-linear interfaces (orthotropic materials).
(7) Generally and as expected, the approach with orthotropic materials and rigid elements provides pushover curves exhibiting both larger initial stiffness and collapse loads. Reasons at the base of such response stand in the larger strength of the orthotropic material used along preferential directions (barrel vault, stone arches when present and spandrels) and the discretization by means of rigid elements and non-linear interfaces, where deformability is concentrated exclusively between adjoining elements.
(8) Softening behavior of the materials has a clear effect on the global pushover curve generally under large displacements of the control node, near the collapse of the structure, see for instance Fig. 13. An approximation with elasto-plastic material without softening is therefore acceptable in this case and may provide accurate predictions of the load bearing capacity of the structure.
(9) The nonsymmetric behavior of the structure and 3D effects are obviously quite evident when dealing with the train load on a single track. In this case, the discrepancy between pushover curves provided by the isotropic and orthotropic FE model are more marked, because the barrel vault works in bending along the transversal direction, where the strength of the equivalent orthotropic material is greater. An additional contribution comes in both load cases (trains on both tracks or on a single track) also from the in-plane strength of the spandrels along the horizontal direction, which is not taken into account in the isotropic model and may explain the discrepancies in the pushover curves obtained, also when dealing with the load case with symmetrical loads.

5. Results of numerical analyses under foundation settlement of a pile

One of the most significant causes of failure for a masonry arch bridge is the differential settlement of piles. A complete list of the potential structural consequences due to loss of support in an arch bridge is provided by McKibbins et al. [50]. When springing remains parallel, the typical settlements that may occur are vertical differential settlement between adjacent supports, horizontal spread of support and horizontal inward movement.

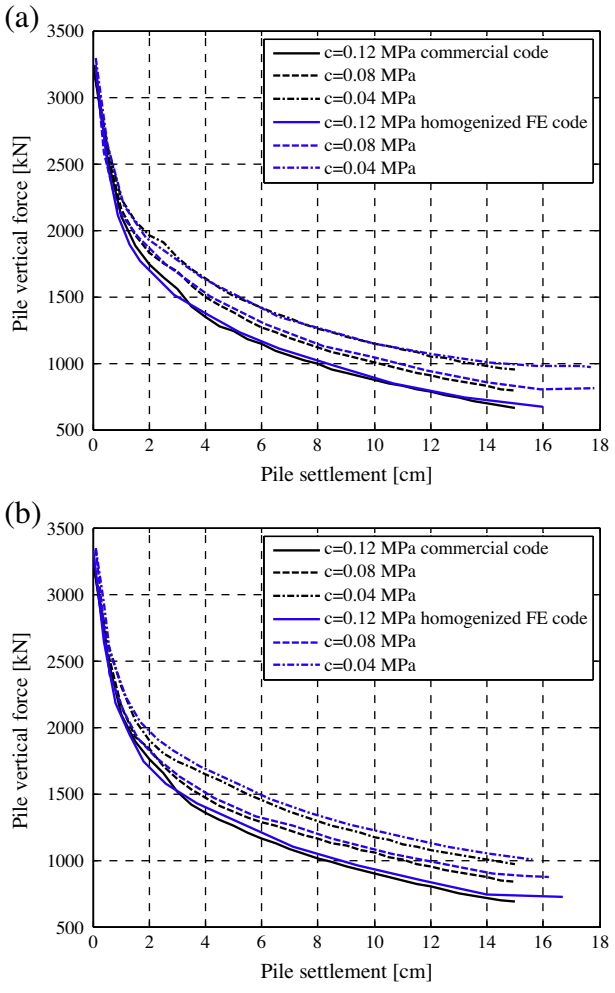

Fig. 23. Right pile settlement. Load displacement curves at different values of infill cohesion at two different friction angles: (a) 30°, and (b) 20°.

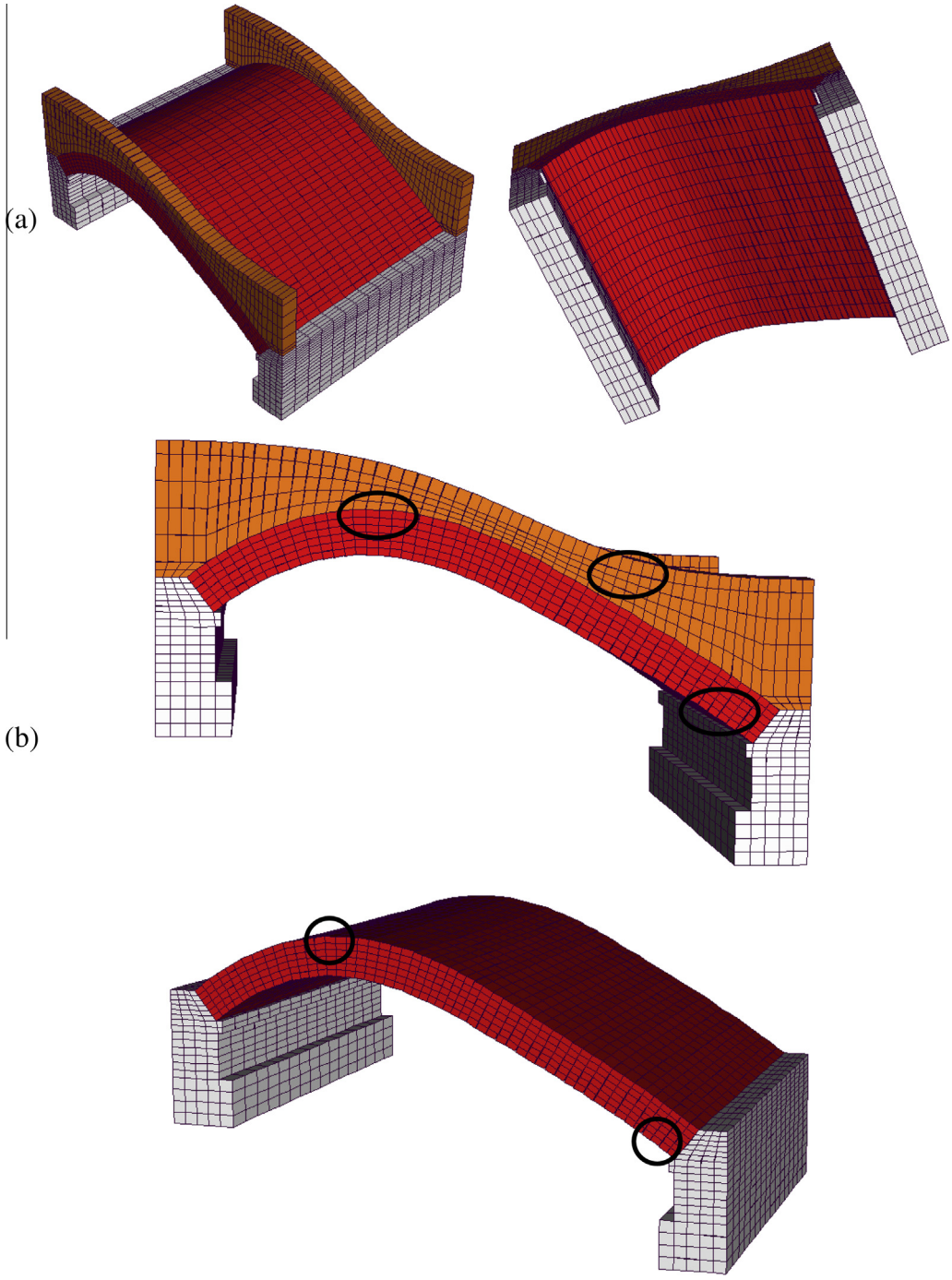

Fig. 24. Right pile settlement. Deformed shape obtained with the non-commercial FE code. (a) Perspective views. (b) Zones where major plasticization occurs, with identification of plastic hinges on the barrel vault.

In these cases, the arch develops three hinges (rarely the arch is able to accommodate support movements with two hinges). If three hinges form and vertical or horizontal settlement continues, then this activates a failure mechanism and should be treated immediately.

In Fig. 23, the load displacement curves obtained when an increasing vertical settlement of the right pile is imposed (under a displacement driven procedure within both FE codes) are shown, at different values of infill cohesion and two different friction angles. For the sake of completeness, in Figs. 24 and 25, the deformed shapes obtained near failure, with a clear visualization of the three hinges forming the failure mechanisms, and obtained by both the non-commercial and commercial software are depicted. In this case, it is quite evident the total absence of transversal 3D effect, as it was easily deducible by the expected failure mechanism. Quite large displacements are required to fully activate the mechanism, meaning that the performance of the bridge under differential settlement is expected to be high. In any case, since the bridge is called to withstand the passage of railway traffic, it should be checked the state of damage under displacement compatible to the passage of a train.

In reality, bridges are often subjected to a combination of different settlements that increases the negative effects of the individual settlements. For instances, a combination of translation

and rotation of the base of a pier causes severe cracking in the arch barrel and in the spandrel walls; settlements of abutments combined with rotation provoke diagonal cracks in the arch barrel. The worst case is when loss of support produces a distortion of the arch barrel which can seriously reduce the load carrying capacity of the bridge. The investigation of all these cases to quantitatively determine the most unfavorable scenario is outside the scopes of the present paper and a specialized wide research program is required in this case. However, it is interesting to notice that the full 3D procedure proposed allows to perform in a quite reliable manner pushover analyses up to failure of the structure, with a computational effort that remains quite reasonable even for relatively complex geometries, as that studied in the present work. As a consequence, at least in principle, it can be affirmed that the software used is capable of provide predictions of the non-linear behavior of a bridge under both a displacement and a force driven framework, efficiently. As a matter of fact, indeed, a single pushover simulation required less than 180 min to be performed on a standard PC equipped with 6 GB RAM and an Intel Core i5 CPU at 2.30 GHz, under common 64 bit Windows 7 OS.

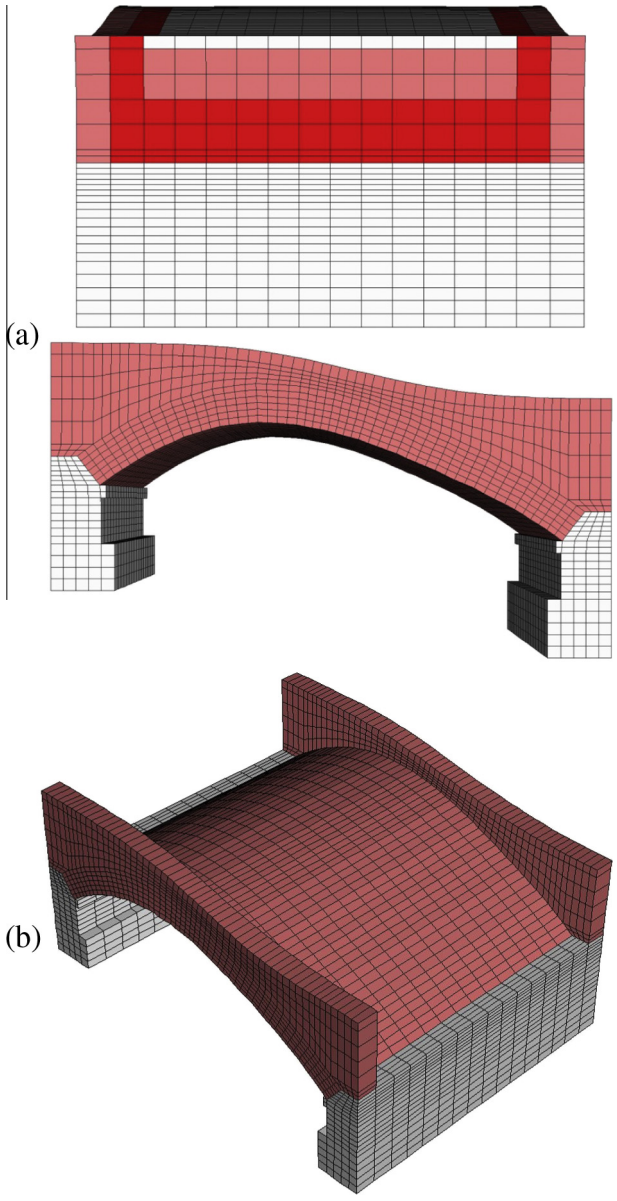

Fig. 25. Right pile settlement. Deformed shape obtained with the commercial FE code. (a) Front and lateral views. (b) Perspective view.

6. Conclusions

Comparative analyses conducted by means of several material models and different software, may be a robust procedure to investigate the behavior at failure and under service loads of historical masonry arch bridges. The analyses conducted in the paper, when considered synoptically, allow to make the following remarks on the case study analyzed:

- The role played by the backfill in increasing the load bearing capacity. A sensitivity analysis is indeed performed changing cohesion and friction angle values and the failure loads so obtained are compared with those predicted in absence of it.
- The role played by the lateral stone arches in both increasing the stiffness and strength of the structure.
- The necessity of 3D analyses for evaluating the nonsymmetric behavior due to the eccentricity of loads and of the structure. In any case, even in presence of symmetric loads, a 3D effect is still present, with larger deformations concentrated in the central part of the structure.
- The role of material characteristics, such as orthotropy and softening of masonry.

The available methods for simulating the behavior of masonry bridge structures resort to different theories or approaches, resulting in: different levels of complexity (from simple graphical methods and hand calculations to complex mathematical formulations and large systems of non-linear equations), different availability for the practitioner, different time requirements (from a few seconds of computer time to many hours of processing) and, of course, different costs. This notwithstanding, this is not a sufficient reason to prefer one method to another. Indeed, a more complex analysis tool does not necessarily provide better results. Most techniques of analysis are adequate, possibly for different applications, if combined with proper engineering reasoning.

As a matter of fact, the results emerged from the analyses allow to conclude that the bridge is safe for the passage of standard trains, whenever the important role of the backfill is not disregarded. However, an experimental mechanical characterization of both backfill and barrel vault would be crucial in the safety assessment of the structure, because the numerical analyses conducted with both the commercial and non-commercial software result rather sensitive to the strength ratio between the different materials constituting the structure. On the other hand, albeit the simplifications intrinsically accepted within the commercial code, it can be stated that results in good agreement with those provided by much more sophisticated approaches have been systematically obtained. The results represent an indirect validation of the elasto-plastic analysis conducted with the commercial code, which at present represents the most refined procedure that can be used in practice, also considering that an experimental characterization of the materials is possible only on models that require a few parameters to set.

Finally, considering that the bridge rests on a soil with very poor mechanical properties, the most useful technical information provided by the paper is the analysis under foundation settlements. From simulation results, it is pretty clear that both a vertical small displacement of the pile could result into unacceptable serviceability conditions, as well as could activate a failure mechanism that is unable to fully utilize the available extra resistance provided by the backfill, as a consequence of the formation of a cylindrical hinge in correspondence of the crown, where the thickness of the backfill is

very low. Obviously, in this latter case 3D effect is not so relevant, as it may occur for differential settlements experienced for bridge piles in rivers, where water floods may be responsible for rotations of the supports.

It is under study by the authors a comprehensive numerical analysis to conduct with alternative approaches based on coupled Finite Element and Discrete Element Methods, in the context of a 2D discretization, to have a full insight into the role played by the combination of a huge amount of input parameters, such as boundary conditions, material properties (especially in the post peak range), loads applied and interaction between contiguous arches.

Acknowledgements

Italian Railways (FFSS) and Prof. Enzo Siviero, who made possible this research on the Venice trans-lagoon bridge, are gratefully acknowledged by the authors.

References

[1] UIC. International Union of Railways: Improving Assessment, Optimization of Maintenance and Development of Database for Masonry Arch Bridges; 2005
[2] Pippard AJS. The approximate estimation of safe loads on masonry bridges. Civil Engineer in war: Institution of Civil Engineers 1948;1:365.
[3] Gilbert M, Melbourne C. Rigid-block analysis to masonry arches. Struct Eng 1994;72:356–61.
[4] Boothby T. Collapse modes of masonry arch bridges. J Brit Mason Soc 1995;9(2):62–9.
[5] Gilbert M. Limit analysis of masonry block structures with non-associative frictional joints using linear programming. Comput Struct 2006;84:873–87.
[6] Gilbert M. Ring: a 2D rigid block analysis program for masonry arch bridges. In: Proc. 3rd international arch bridges conference, Paris, France; 2001: 109–118.
[7] de Felice G, De Santis S. Experimental and numerical response of arch bridge historic masonry under eccentric loading. Int J Architect Heritage 2010;4(2):115–37.
[8] Audenaert A, Fanning P, Sobczak L, Peremans H. 2-D analysis of arch bridges using an elasto-plastic material model. Eng Struct 2008;30:845–55.
[9] Lourenço PB, Milani G, Tralli A, Zucchini A. Analysis of masonry structures: review of and recent trends in homogenisation techniques. Can J Civ Eng 2007;34(11):1443–57.
[10] Oliveira DV, Lourenço PB, Lemos C. Geometric issues and ultimate load of masonry arch bridges from the northwest Iberian Peninsula. Eng Struct 2010;32(12):3955–65.
[11] Cavicchi A, Gambarotta L. Collapse analysis of masonry bridges taking into account arch-fill interaction. Eng Struct 2005;27(4):605–15.
[12] Cavicchi A, Gambarotta L. Two-dimensional finite element upper bound limit analysis of masonry bridges. Comput Struct 2006;84(31–32):2316–28.
[13] Cavicchi A, Gambarotta L. Upper bound limit analysis of multispan masonry bridges including arch-fill interaction. In: Roca P, Molins C, editors. Arch Bridges IV – Advances in Assessment, Structural Design and Construction, Barcelona; 2004. p. 302–311.
[14] Cavicchi A, Gambarotta L. Load carrying capacity of masonry bridges: numerical evaluation of the influence of fill and spandrels, In: Lourenço PB, Oliveira DV, Portela A, editors. Proceedings of the Arch'07 – 5th International Conference on Arch Bridges, 12–14 September 2007, Madeira; 2007. p. 609–616.
[15] Milani G, Lourenço PB. 3D non-linear behavior of masonry arch bridges. Comput Struct 2012;110–111:133–50.
[16] Milani G, Tralli A. Simple SQP approach for out-of-plane loaded homogenized brickwork panels accounting for softening. Comput Struct 2011;89(1–2):201–15.
[17] Drosopoulos GA, Stavroulakis GE, Massalas CV. Limit analysis of a single span masonry bridge with unilateral frictional contact interfaces. Eng Struct 2006;28(13):1864–73.
[18] Brencich A, Morbiducci R. Masonry arches: historical rules and modern mechanics. Int J Architect Heritage 2007;1(2):165–89.
[19] Pippard AJS, Ashby ERJ. An experimental study of the voissour arch. J Inst Civ Eng 1936;10:383–403.
[20] Heyman J. The safety of masonry arches. Int J Mech Sci 1969;43:209–24.
[21] Hughes TG, Blackler MJ. A review of the UK masonry arch assessment methods. Proc Inst Civ Eng 1997;122:305–15.
[22] Fanning PJ, Boothby TE. Three dimensional modelling and full scale testing of stone arch bridges. Comput Struct 2001;79(29–30):2645–62.
[23] Fanning PJ, Boothby TE, Roberts BJ. Longitudinal and transverse effects in masonry arch assessment. Constr Build Mater 2001;15(1):51–60.
[24] Zeman J, Nováka J, Šejnoha M, Šejnoha J. Pragmatic multi-scale and multi-physics analysis of Charles Bridge in Prague. Eng Struct 2008;30(11):3365–76.
[25] Cecchi A, Milani G, Tralli A. Validation of analytical multiparameter homogenisation models for out-of-plane loaded masonry walls by means of Finite Element method. ASCE J Eng Mech 2005;131(2):185–98.
[26] Reccia E. Conservation of masonry arch bridges. A procedure for modelling and strengthening, PhD Dissertation, ETCAEH, UNG; 2013.
[27] Huerta S. Mechanics of masonry vaults: the equilibrium approach. In: Lourenço PB, Roca P, editors. Proc. Historical Constructions, Guimarães PT; 2001.
[28] Luciano R, Sacco E. Homogenisation technique and damage model for old masonry material. Int J Solids Struct 1997;34(24):3191–208.
[29] Massart T, Peerlings RHJ, Geers MGD. Mesoscopic modeling of failure and damage-induced anisotropy in brick masonry. Eur J Mech A/Solids 2004;23:719–35.
[30] Mercatoris BCN, Massart TJ, Bouillard P. Multi-scale detection of failure in planar masonry thin shells using computational homogenization. Eng Fract Mech 2009;76(4):479–99.
[31] Milani G, Milani E, Tralli A. Upper Bound limit analysis model for FRP-reinforced masonry curved structures. Part II: structural analyses. Comput Struct 2009;87(23–24):1534–58.
[32] Milani G, Lourenco PB, Tralli A. Homogenised limit analysis of masonry walls. Part I: failure surfaces. Comput Struct 2006;84(3–4):166–80.
[33] Milani G, Lourenco PB, Tralli A. Homogenization approach for the limit analysis of out-of-plane loaded masonry walls. Homogenised limit analysis of masonry walls. Part II: structural examples. Comput Struct 2006;84(3–4):181–95.
[34] STRAUS7®. Theoretical manual-theoretical background to the Strand7 Finite Element analysis system; 2004.
[35] Lourenço PB, Krakowiak KJ, Fernandes FM, Ramos LF. Failure analysis of Monastery of Jeronimos, Lisbon: How to learn from sophisticated numerical models. Eng Fail Anal 2007;14:280–300.
[36] Milani G. Simple homogenization model for the non-linear analysis of in-plane loaded masonry walls. Comput Struct 2011;89:1586–601.
[37] Torre C. Dizionario storico dei ponti ad arco in muratura. Firenze: Alinea; 2003.
[38] Di Tommaso A, Barbieri A, Chiaradia V. Railway masonry arch bridge of Venice lagoon: history, technology and structural behaviour, In: Proc. ARCH'04, Barcelona, Spain; 2004.
[39] Reccia E, Cecchi A, Tralli A. Homogenization of Masonry Vault Bridges: Sensitivity to External Stone Arch. In: proc. of 14th International Conference on Civil, Structural and Environmental Engineering Computing, CC2013; Cagliari, Sardinia, Italy: 2013.
[40] Cecchi A, Sab K. A multi-parameter homogenization study for modeling elastic masonry. Eur J Mech A/Solids 2002;21:249–68.
[41] Cecchi A, Sab K. A comparison between a 3D discrete model and two homogenized plate models for periodic elastic brickwork. Int J Solids Struct 2004;41:2259–76.
[42] Italian Railway Code, N° I/SC/PS-OM/2298. 2nd June 1995. updated 13th January 1997.
[43] Craemer H. Die "erzwungene Drucklinie" als Ausdruck der versteifenden Wirkung der Übermauerung von Gewölben, Beton und Stahlbetonbau, Heft 9/10; 1943.
[44] Herzog R. Wechselbeziehungen zwischen Bogen und Bogenüberbauten von Brücken. Moskau: Technisch-Wissenschaftlicher Verlag des Ministeriums für Automobiltransport und Chaussee-Straßen der RSFSR; 1962.
[45] Bienert G. Aufgaben der Modellstatik bei der Konstruktion und Unterhaltung der Verkehrsbauwerke, Wissenschaftliche Zeitschrift der Hochschule für Verkehrswesen; Friedrich List, Dresden, Hesk 1; 1959–60.
[46] Brencich A, Colla C. The influence of construction technology on the mechanics of masonry railway bridges. In: Proc. Railway Engineering 2002, 5th International Conference, London 3–4 July; 2002.
[47] Smith CC, Gilbert M, Callaway PA. Geotechnical issues in the analysis of masonry arch bridges, In: Roca P, Molin C, editors. Arch Bridges IV – Advances in Assessment, Structural Design and Construction, 2004. p. 344–352.
[48] Molins C, Roca P. Capacity of masonry arches and spatial structures. J Struct Eng ASCE 1998;124(6):653–63.
[49] Milani G. 3D upper bound limit analysis of multi-leaf masonry walls. Int J Mech Sci 2008;50(4):817–36.
[50] Mc Kibbins L, Melbourne C, Sawar N, Sicilia C. Masonry arch bridges: condition appraisal and remedial treatment. London: Ciria, C656; 2006.